Synthesis and C–C Coupling Reactivity of a Dinuclear Ni^{I}–Ni^{I} Complex Supported by a Terphenyl Diphosphine

Alexandra Velian, Sibo Lin, Alexander J. M. Miller, Michael W. Day, and Theodor Agapie*

Division of Chemistry and Chemical Engineering, Arnold and Mabel Beckman Laboratories of Chemical Synthesis, California Institute of Technology, Pasadena, California 91125

Supporting Information

Experimental Details

Proposed Mechanisms

Crystallographic Information

Experimental Details

General considerations. All air- and moisture-sensitive compounds were manipulated using standard vacuum line, Schlenk, or cannula techniques or in a glove box under a nitrogen atmosphere. Solvents for air- and moisture-sensitive reactions were dried over sodium benzophenone ketyl, calcium hydride, or by the method of Grubbs.[1] Acetonitrile-d_3 and dichloromethane-d_2, were purchased from Cambridge Isotopes and distilled from calcium hydride. Benzene-d_6 was also purchased from Cambridge Isotope Laboratories, Inc. and distilled from sodium benzophenone ketyl. Other materials were used as received. UV-Vis measurements were taken on a Varian Cary 50 spectrophotometer using a quartz crystal cell. ^{1}H, ^{13}C, and ^{31}P NMR spectra were recorded on Varian Mercury 300 or Varian INOVA-500 spectrometers at room temperature, unless indicated otherwise. Chemical shifts are reported with respect to internal solvent: 7.16 ppm, and 128.06 (t) ppm (C_6D_6) for ^{1}H and ^{13}C NMR data. ^{31}P NMR chemical shifts are reported with respect to an external 85% H_3PO_4 reference (0 ppm). Gas chromatography-mass spectrometry (GC-MS) analysis was performed upon treating reaction mixtures with methanol and filtering through a plug of silica gel. GC peaks were initially identified by a good (>90%) match with an entry from the "PBM Quick Search" database and confirmed by comparison to an authentic sample. Fast atom bombardment-mass spectrometry (FAB-MS) analysis was performed with a JEOL JMS-600H high resolution mass spectrometer. Elemental analysis was conducted by Midwest Microlab, LLC (Indianapolis, IN).

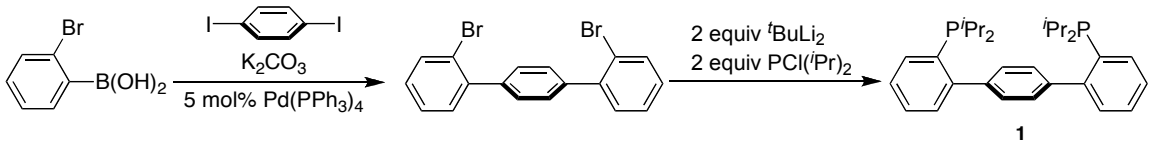

Synthesis of 1,4-bis(2-bromophenyl)benzene. Suzuki coupling conditions were adapted from a previously published procedure.[2] 1,4-diiodobenzene (3.90 g, 11.82 mmol, 1 equiv), 2-bromo-phenylboronic acid (5.00 g, 24.89 mmol, 2.1 equiv), K_2CO_3 (9.80 g, 70.90 mmol, 6 equiv), 270 mL toluene, 65 mL ethanol, and 65 mL water were added to a 500 mL Schlenk tube fitted with a screw-in Teflon stopper. The mixture was degassed by

two freeze-pump-thaw cycles, and $Pd(PPh_3)_4$ (685 mg, 0.59 mmol, 0.05 equiv) was added with a counterflow of nitrogen. The reaction vessel was placed in an oil bath preheated at 65 °C. After stirring for 18 h the mixture was allowed to cool to room temperature. Volatiles were removed via rotary evaporation and water was added. This mixture was extracted with CH_2Cl_2 (three times). The combined organic fractions were dried over $MgSO_4$, filtered, and concentrated via rotary evaporation. Recrystallization from CH_2Cl_2/MeOH followed by filtration and drying garnered 2.8 g (60% yield, 11.07 mmol) of pale yellow crystals. ^{1}H NMR (300 MHz, C_6D_6) δ: 7.49 (dd, *J* = 8.0, 1.2 Hz, 2H, aryl-*H*), 7.35 (s, 4H, central aryl-*H*), 7.08 (dd, *J* = 8.0, 1.7 Hz, 2H, aryl-*H*), 6.95 (td, *J* = 7.5, 1.2Hz, 2H, aryl-*H*), 6.76 (td, *J* = 7.5, 1.7 Hz, 2H, aryl-*H*). $^{13}C\{^1H\}$ NMR (75 MHz, C_6D_6) δ: 142.66, 140.72, 133.49, 131.71, 129.46, 129.03, 127.58, 123.01. The ^{1}H NMR spectrum in $CDCl_3$ matched previously published data.[3] MS (m/z): calcd, 387.9285 (M^+); found 388 (GC-MS, M^+), 387.9301 (FAB-MS, M^+).

Synthesis of 1,4-bis(2-(diisopropylphosphino)phenyl)benzene (**1**). A mixture of 1,4-bis(2-bromophenyl)benzene (2.25 g, 5.79 mmol, 1 equiv) and THF (40 mL) in a Schlenk tube fitted with a screw-in Teflon stopper was frozen in a cold well, in an inert atmosphere glove box. This mixture was allowed to thaw and ^{t}BuLi solution (1.7 M in pentanes, 14 mL, 23.77 mmol, 4.1 equiv) was added via syringe while thawing. This purple-grey mixture was stirred for 30 min allowing it to reach room temperature. Chlorodiisopropylphosphine (1.86 g, 12.19 mmol, 2.1 equiv) was added via syringe to the reaction mixture, which within minutes became a yellow-brown solution. After stirring at room temperature for 3 h, the volatiles were removed and the residue was dissolved in toluene and filtered through Celite. The volatiles were removed from the eluent under reduced pressure, and the resulting solids were washed with cold diethyl ether (20 ml) and filtered to yield 1.76 g (65% yield, 3.80 mmol) of spectroscopically pure **1** as a white solid. ^{1}H NMR (300 MHz, C_6D_6) δ: 7.55 (s, 4H, central aryl-*H*), 7.47 – 7.40 (m, 2H, aryl-*H*), 7.34 – 7.26 (m, 2H, aryl-*H*), 7.20-7.13 (m, 4H, aryl-*H*), 1.88 (m, 4H, C*H*$(CH_3)_2$), 1.05 – 0.88 (m, 24H, CH(C*H*$_3)_2$). $^{13}C\{^1H\}$ NMR (75 MHz, C_6D_6) δ: 150.81 (d, *J* = 27.5 Hz), 141.44 (d, *J* = 5.5 Hz), 135.17 (d, *J* = 24.2 Hz), 132.77 (d, *J* = 2.9 Hz), 131.01 (d, *J* = 5.2 Hz), 130.57 (d, *J* = 5.1 Hz), 128.66 (s), 126.77 (s), 24.88 (d, *J*

= 16.1 Hz), 20.48 (d, J = 20.0 Hz), 19.85 (d, J = 11.3 Hz). $^{31}P\{^{1}H\}$ NMR (75 MHz, C_6D_6) δ: -4.7. MS (m/z): calcd, 462.2605 (M^+); found, 461 (GC-MS, M^+), 463.2665 and 479.2661 (FAB-MS, $[M+H]^+$ and $[M+O+H]^+$). Unfortunately, samples of **1** could not be subjected to FAB-MS under rigorously air-free conditions, and partial monooxygenation was observed.

Synthesis of [1,4-bis{2-(diisopropylphosphino)phenyl}benzene]nickel(0) (2).

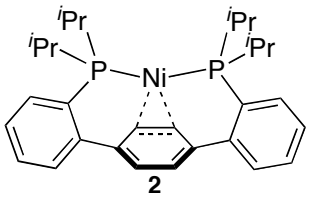

2

Upon addition of $Ni(COD)_2$ (0.24 g, 0.864 mmol) to a colorless solution of **1** (0.4 g, 0.864 mmol) in THF (20 mL), the color of the mixture changed to deep red. The mixture was stirred at room temperature for 1 h. The volatiles were removed under reduced pressure to yield a deep red powder. X-ray quality crystals were grown in hexamethyldisiloxane at -35 °C. ^{1}H NMR (300 MHz, C_6D_6) δ: 7.61-7.60 (m, 2H, aryl-*H*), 7.35 (m, 2H, aryl-*H*), 7.22-7.19 (m, 4H, aryl-*H*), 5.52 (broad, 4H, central aryl-*H*), 2.02 (broad, 4H, C*H*$(CH_3)_2$), 1.14-1.09 (m, 12H, CH(C*H*$_3)_2$) and 1.2- 0.8 (m, 12H, CH(C*H*$_3)_2$). $^{13}C\{^{1}H\}$ NMR (75 MHz, C_6D_6) δ: 152.12 (t, J = 8.1 Hz), 132.86 (t, J = 2.2 Hz), 131.11 (s), 129.31 (s), 128.84 (s), 128.59 (s), 127.16 (t, J = 2.1 Hz), 126.65 (t, J = 1.3 Hz), 27.10 (t, J = 6.8 Hz), 20.40 (t, J = 5.6 Hz), 19.96 (s, broad). $^{31}P\{^{1}H\}$ NMR (75 MHz, C_6D_6) δ: 40.4. Anal. Calcd. For $C_{30}H_{40}NiP_2$ (%): C, 68.69; H, 7.61. Found: C, 69.12; H, 7.73. λ_{max} (THF, nm), ε (M^{-1} cm^{-1}): 256, 1.51 x 10^4; 396, 5.37 x 10^3; 494, 2.40 x 10^3.

Synthesis of [1,4-bis{2-(diisopropylphosphino)phenyl}benzene]-bis(μ-chloro)dinickel(I) (3) from 1.

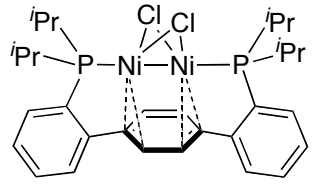

3

Upon addition of $Ni(COD)_2$ (0.332 g, 1.51 mmol) and $NiCl_2$(dme) (0.416 g, 1.51 mmol) to a colorless solution of **1** (0.700 g, 1.51 mmol) in THF (50 mL), the color of the mixture changes first to red and then to green. The mixture is stirred at room temperature for 30 min, and the volatiles removed under reduced pressure. Recrystallization from a concentrated benzene solution procured X-ray quality crystals of **3** • C_6H_6. Alternatively, recrystallization from THF/pentane at -35 °C gave **3** in 90% yield. ^{1}H NMR (300 MHz, C_6D_6) δ: 7.24 (d, *J* = 7.5 Hz, 2H, aryl-*H*), 6.99 (app t, 2H, aryl-*H*), 6.87 (app t, 2H, aryl-*H*), 6.74 (s, 4H, central aryl-*H*), 6.69 (br d, 2H, aryl-*H*), 1.5 (m, 4H, C*H*$(CH_3)_2$), 1.25 (app d, 12H, CH(C*H*$_3)_2$), 0.91 (app d, 12H, CH(C*H*$_3)_2$). ^{13}C{^{1}H} NMR (75 MHz, C_6D_6) δ: 154.07 (t, *J* = 10.0 Hz), 133.73 (t, *J* = 16.4 Hz), 130.62 (s), 130.42 (s), 129.70 (s), 126.92 (s), 104.35 (s), 89.78 (s), 23.08 (t, *J* = 8.6 Hz), 19.03 (s), 18.06 (s). ^{31}P{^{1}H} NMR (75 MHz, C_6D_6) δ: 47.3. Anal. Calcd. For $C_{30}H_{40}Cl_2Ni_2P_2$ (%): C, 55.36; H, 6.19. Found: C, 54.92; H, 6.47. λ_{max} (THF, nm), ε (M^{-1} cm^{-1}): 249, 3.75 x 10^4; 318, 3.21 x 10^4; 375, 8.01 x 10^3; 446, 8.52 x 10^3; 739, 7.68 x 10^2.

Synthesis of 3 from 2. $NiCl_2$(dme) (0.042 g, 0.15 mmol) was added to a red solution of **2** (0.033 g, 0.15 mmol) in THF (5 mL) and stirred for 30 minutes to give a dark green solution. Volatiles were removed under reduced pressure, and ^{1}H and ^{31}P NMR spectroscopy identified the sole product as **3**.

Synthesis of [1,4-bis{2-(diisopropylphosphino)phenyl}benzene][biphenyl(2, 2')diyl]dinickel(I) (4).

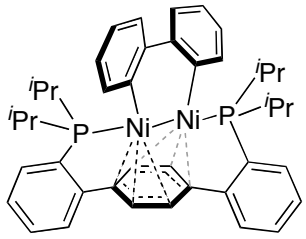

4

Magnesium turnings (100 mg), 2,2'-dibromobiphenyl (101 mg, 0.32 mmol, 1 equiv), and THF (15 mL) were heated in a Schlenk flask at 40 °C. After 4h, an aliquot was quenched with D_2O, dried with $MgSO_4$, and filtered through silica gel. GC-MS analysis of the aliquot showed the absence of starting 2,2'-dibromobiphenyl and the presence of d_2-biphenyl, indicating the complete conversion of starting material to Grignard. The solution was filtered through Celite to remove magnesium particles. Solvent was removed under reduced pressure to yield an off-white powder that was suspended in toluene (50 mL) and frozen in a cold well. A solution of **3** (234.3 mg, 0.32 mmol, 1 equiv) in toluene (15 mL) was chilled to -35 °C and layered on top of the frozen Grignard solution. The reaction mixture was frozen solid, then allowed to thaw and stir for 40 minutes, during which the solution gradually changed from dark green to dark brown. Volatile materials were removed under reduced pressure, and the residue was dissolved in hexanes (50 mL) and filtered through Celite. The filtrate was concentrated under reduced pressure, and the residue was washed with hexanes (20 mL). The wash was discarded by filtration, while the remaining residue was dissolved in hexanes (50 mL) and filtered again. The filtrate was concentrated to a residue under reduced pressure, and lyophilized in benzene to obtain a brown powder (39.1 mg, 0.05 mmol, 27%). A concentrated solution of **4** in hexanes was chilled to -35 °C for 1 day to yield X-ray quality crystals. ^{1}H NMR (300 MHz, C_6D_6) δ: 7.56 (d, 2H, aryl-*H*), 7.43 (d, 2H, aryl-*H*), 7.23 (d, 2H, aryl-*H*), 7.07-6.90 (m, 10H, aryl-*H*), 5.26 (s, 4H, central aryl-*H*), 1.92 (m, 4H, C*H*(CH_3)$_2$), and 0.69 (m, 24H, CH(C*H*$_3$)$_2$). ^{13}C{^{1}H} NMR (300 MHz, C_6D_6) δ: 164.18 (s), 163.40 (t, J = 3.4 Hz), 152.24 (t, J = 15.2 Hz), 138.93 (s), 138.62 (t, J = 12.5 Hz), 131.35 (s), 129.69 (s), 128.88 (t, J = 5.8 Hz), 127.46 (s), 123.92 (s), 123.38 (s), 121.72 (s), 92.18 (s), 88.92 (s), 25.25 (s), and 17.89 (s). ^{31}P{^{1}H} NMR (300 MHz, C_6D_6)

δ: 36.9. Anal. Calcd. For $C_{30}H_{40}Cl_2Ni_2P_2$ (%): C, 68.90; H, 6.61. Found: C, 69.01; H, 6.54. λ_{max} (C_6H_6, nm), ε (M^{-1} cm^{-1}): 439, 3.9 x 10^2; 518, 2.6 x 10^2; 665, 7.2 x 10^1.

Reaction of 3 with PhMgBr. A 20 mL vial was charged with a stir bar and a solution of **3** (64 mg, 0.10 mmol) in THF (2 mL). This mixture was frozen in a cold well. PhMgBr (0.89 M in THF, 0.12 mL, 0.10 mmol) was added to the thawing reaction mixture. The reaction was stirred at room temperature for an hour, during which the reaction mixture changed from dark green to dark brown. GC-MS analysis revealed biphenyl as the major organic product.

Reaction of 4 with CO. A 100 mL Schlenk flask was charged with a stir bar and a solution of **4** (98 mg, 0.13 mmol) in C_6H_6 (15 mL) inside a nitrogen-atmosphere glovebox and covered with a rubber septum. The flask was brought out of the box, and CO (19.3 mL, 0.80 mmol) was injected into the solution with a syringe and long metal needle. Over 15 min the reaction mixture changed from dark brown to pale green-yellow. The reaction was placed under a positive nitrogen pressure while the septum was replaced with a greased glass stopper, and then volatiles were removed under vacuum. The solid was dissolved in hexanes and filtered through Celite. Volatiles were again removed under vacuum, and the resultant yellow solid was triturated in hexanes and filtered through Celite. The filtrate was found by ^{1}H-NMR and GC-MS to contain fluorenone. The filter cake was collected by washing with more hexanes. NMR spectra of the filter cake were complex but contained well-defined features. ^{1}H NMR (300 MHz, C_6D_6) δ: 8.34 – 8.20 (m, 2.33H), 8.09 – 8.01 (m, 0.22H), 7.86 (d, *J* = 7.3 Hz, 0.60), 7.13 (s, 5.44H), 7.10 – 6.76 (m, 15.09H), 6.71 (app d, 0.75H), 5.85 (s, 1.00H), 5.65 (s, 0.13H), 4.56 (s, 0.12H), 3.58 (m, 0.13H), 2.32 (m, 1.65H), 2.10 (m, 6.02H), 1.04 (d, *J* = 6.7 Hz, 11.50H), 0.98 (d, *J* = 6.7 Hz, 10.03H), 0.81 (d, *J* = 6.9 Hz, 11.25H), 0.76 (d, *J* = 6.9 Hz, 8.03H). ^{31}P{^{1}H} NMR (300 MHz, C_6D_6) δ: 75.0 (broad), 51.1, 50.1, 38.1 (broad), 37.1, 35.6. Hexanes was layered on a concentrated solution of this mixture in Et_2O to yield yellow-orange crystals that were found to be a mixture of nickel carbonyls, **5**: ca. 80% of the phosphines are bound to nickel dicarbonyl and the remaining phosphines are bound to nickel tricarbonyl.

Reaction of 4 with CH_2Cl_2. A C_6D_6 (0.6 mL) solution of **4** (10 mg, 0.01 mmol) was transferred to a J. Young NMR tube. 5 drops of CH_2Cl_2 were added and the reaction was followed by ^{31}P NMR spectroscopy. At 3.75 h, the reaction was complete and had changed from dark brown to dark green in color. ^{1}H and ^{31}P NMR spectra identified **3** as the major organometallic species in solution. GC-MS analysis of the crude mixture indicated thatfluorene was the only organic species present.

Proposed Mechanisms

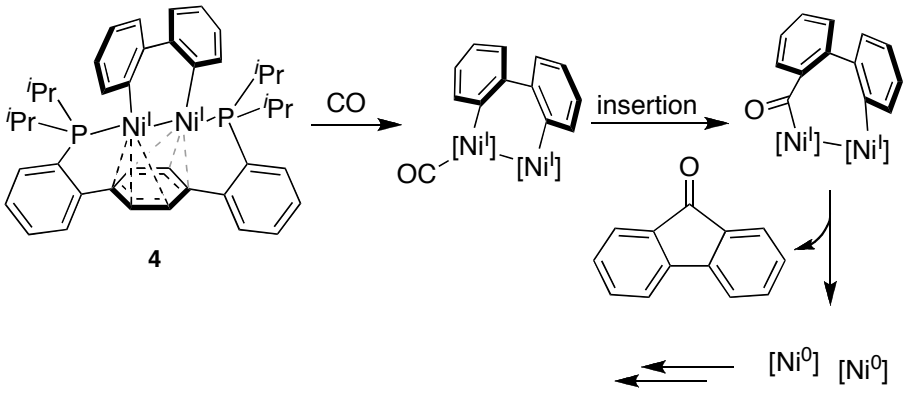

Scheme 1. Proposed mechanism for fluorenone formation from **4** and carbon monoxide.

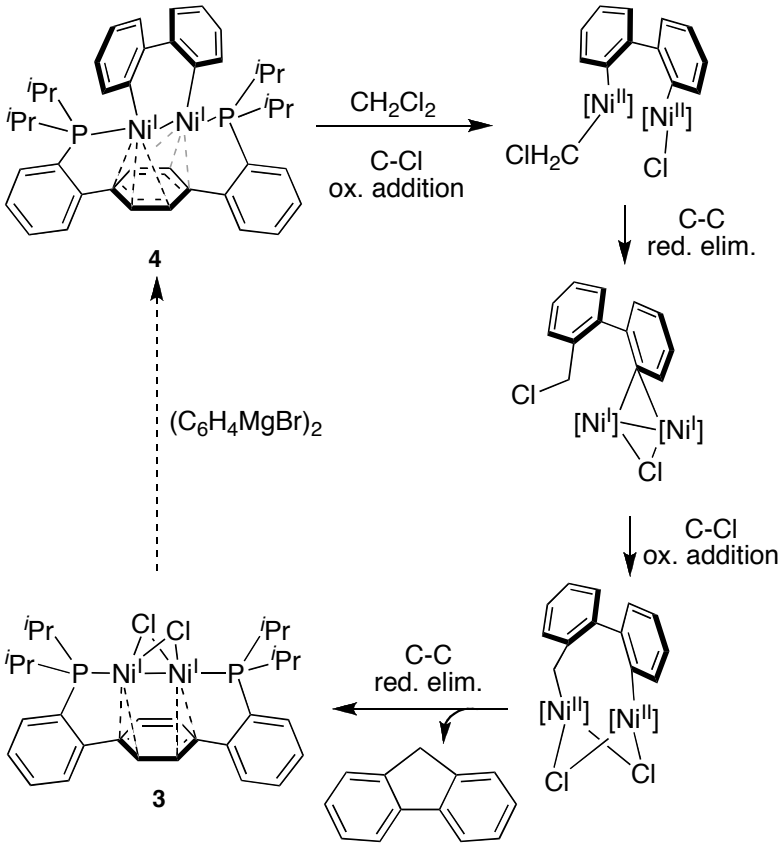

Scheme 2. Proposed mechanism for fluorene formation from **4** and dichloromethane.

Crystallographic Information

Reported bending angles between the central and peripheral arenes were measured from the angle defined by the two *ipso*-carbons of the central arene and the adjoining carbon of a peripheral arene.

Crystallographic data have been deposited at the CCDC, 12 Union Road, Cambridge CB2 1EZ, UK and copies can be obtained on request, free of charge, by quoting the publication citation and the deposition numbers 745169, 702807, 745065, and 767040.

Table 2. Crystal and refinement data for **2**, **3**, **4**, and **5**

	2	**3**	**4**	**5**
empirical formula	$C_{30}H_{40}P_2Ni$	$C_{30}H_{40}P_2Cl_2Ni_2 \bullet C_6H_6$	$C_{42}H_{48}P_2Ni_2 \bullet ½ (C_6H_{14})$	$0.80(C_{34}H_{40}O_4P_2Ni_2)$ $0.20(C_{36}H_{40}O_6P_2Ni_2)$
formula wt	521.27	728.99	775.25	703.36
T (K)	100(2)	100(2)	100(2)	100(2)
a, Å	8.5770(3)	9.6730(5)	11.7255(5)	7.1846(13)
b, Å	14.8684(5)	12.8755(6)	13.1876(5)	25.477(4)
c, Å	21.6483(7)	14.3392(7)	14.7366(6)	9.4217(16)
α, deg	90	102.753(3)	105.066(2)	90
β, deg	90	99.036(3)	97.410(2)	100.794(11)
γ, deg	90	91.500(3)	115.216(2)	90
V, $Å^3$	2760.73(16)	1716.76(15)	1814.32(13)	1694.1(5)
Z	4	2	2	2
cryst syst	orthorhombic	triclinic	triclinic	monoclinic
space group	$P2_12_12_1$	P-1	P-1	$P2_1/n$
d_{calcd}, g/cm^3	1254	1410	1345	1379
θ range, deg	1.66−35.07	1.93−45.99	1.49−39.07	2.34−26.37
μ, mm^{-1}	0.835	1.37	1.098	1.242
abs cor	none	semi-empirical from equivalents	none	semi-empirical from equivalents
GOF	1.311	2.237	1.747	1.248
R1,[a] wR2[b] (I > 2σ(I))	0.0302, 0.0568	0.0270, 0.0532	0.0334, 0.0565	0.0651, 0.0634

[a] $R1 = \sum||F_o| - |F_c||/\sum|F_o|$. [b] $wR2 = \{\sum[w(F_o^2 - F_c^2)^2]/\sum[w(F_o^2)^2]\}^{1/2}$.

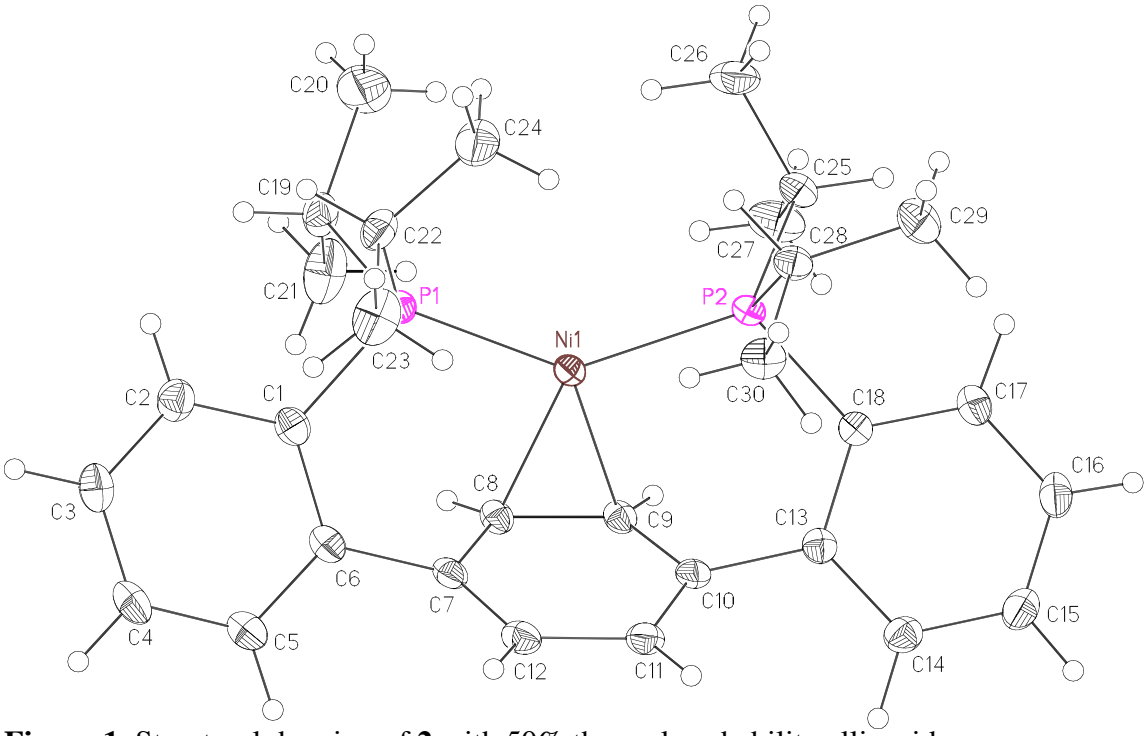

Figure 1. Structural drawing of **2** with 50% thermal probability ellipsoids.

Special refinement details for 2. Crystals were mounted on a glass fiber using Paratone oil then placed on the diffractometer under a nitrogen stream at 100K. Refinement of F^2 against ALL reflections. The weighted R-factor (*w*R) and goodness of fit (S) are based on F^2, conventional R-factors (R) are based on F, with F set to zero for negative F^2. The threshold expression of $F^2 > 2\sigma(F^2)$ is used only for calculating R-factors(gt) etc. and is not relevant to the choice of reflections for refinement. R-factors based on F^2 are statistically about twice as large as those based on F, and R-factors based on ALL data will be even larger. All esds (except the esd in the dihedral angle between two l.s. planes) are estimated using the full covariance matrix. The cell esds are taken into account individually in the estimation of esds in distances, angles and torsion angles; correlations between esds in cell parameters are only used when they are defined by crystal symmetry. An approximate (isotropic) treatment of cell esds is used for estimating esds involving l.s. planes.

Table 3. Atomic coordinates (x 10^4) and equivalent isotropic displacement parameters ($Å^2$x 10^3) for **2**. U(eq) is defined as the trace of the orthogonalized U^{ij} tensor.

	x	y	z	U_{eq}
Ni(1)	3714(1)	5309(1)	1370(1)	14(1)
P(1)	3794(1)	6351(1)	2076(1)	15(1)
P(2)	3436(1)	5299(1)	371(1)	14(1)
C(1)	4955(2)	6004(1)	2758(1)	18(1)
C(2)	5030(2)	6568(1)	3277(1)	23(1)
C(3)	6020(2)	6374(1)	3768(1)	26(1)
C(4)	6972(2)	5624(1)	3743(1)	25(1)
C(5)	6924(2)	5057(1)	3233(1)	22(1)
C(6)	5896(2)	5226(1)	2744(1)	18(1)
C(7)	5815(2)	4618(1)	2202(1)	16(1)
C(8)	4277(2)	4375(1)	1998(1)	16(1)
C(9)	4089(2)	3988(1)	1399(1)	15(1)
C(10)	5439(2)	3849(1)	1022(1)	16(1)
C(11)	6910(2)	3985(1)	1258(1)	18(1)
C(12)	7093(2)	4382(1)	1859(1)	19(1)
C(13)	5136(2)	3662(1)	359(1)	16(1)
C(14)	5855(2)	2936(1)	62(1)	20(1)
C(15)	5485(2)	2724(1)	-546(1)	23(1)
C(16)	4390(2)	3229(1)	-861(1)	23(1)
C(17)	3706(2)	3974(1)	-580(1)	20(1)
C(18)	4097(2)	4218(1)	27(1)	15(1)
C(19)	1907(2)	6612(1)	2459(1)	24(1)
C(20)	845(2)	7214(2)	2073(1)	44(1)
C(21)	1099(2)	5738(1)	2638(1)	35(1)
C(22)	4673(2)	7483(1)	1926(1)	22(1)
C(23)	6450(2)	7429(1)	1952(1)	32(1)
C(24)	4180(3)	7832(1)	1292(1)	32(1)
C(25)	1446(2)	5450(1)	56(1)	18(1)
C(26)	900(2)	6414(1)	186(1)	28(1)
C(27)	360(2)	4762(1)	342(1)	29(1)
C(28)	4629(2)	6124(1)	-72(1)	18(1)
C(29)	4454(2)	6123(1)	-776(1)	26(1)
C(30)	6327(2)	6027(1)	117(1)	23(1)

Table 4. Anisotropic displacement parameters ($Å^2 x\ 10^4$) for **2**. The anisotropic displacement factor exponent takes the form: $-2\pi^2[\ h^2 a^{*2} U^{11} + ... + 2\ h\ k\ a^*\ b^*\ U^{12}\ ]$

	U^{11}	U^{22}	U^{33}	U^{23}	U^{13}	U^{12}
Ni(1)	144(1)	145(1)	126(1)	12(1)	-9(1)	4(1)
P(1)	155(2)	167(1)	140(1)	3(1)	0(1)	10(1)
P(2)	143(2)	137(1)	136(1)	22(1)	-11(1)	4(1)
C(1)	165(7)	205(6)	171(5)	5(4)	-21(5)	-29(5)
C(2)	222(7)	240(6)	217(6)	-39(5)	-8(6)	-7(6)
C(3)	289(8)	301(6)	185(5)	-47(5)	-29(6)	-33(6)
C(4)	268(8)	292(6)	180(6)	23(5)	-81(6)	-24(6)
C(5)	226(7)	222(6)	205(5)	37(4)	-47(6)	-16(5)
C(6)	182(6)	184(5)	164(4)	28(4)	-24(5)	-29(5)
C(7)	196(6)	137(5)	155(4)	30(4)	-43(5)	2(5)
C(8)	181(7)	156(5)	140(5)	25(4)	-7(5)	-11(5)
C(9)	174(6)	130(4)	148(4)	18(4)	-17(5)	-18(4)
C(10)	201(7)	121(5)	162(5)	26(4)	-18(5)	19(5)
C(11)	166(7)	185(5)	198(5)	15(4)	-11(5)	31(5)
C(12)	168(7)	191(5)	215(6)	15(4)	-50(6)	7(5)
C(13)	177(7)	148(5)	158(5)	15(4)	8(5)	-20(5)
C(14)	218(7)	179(5)	203(5)	19(4)	33(5)	16(5)
C(15)	315(9)	170(5)	198(6)	-2(4)	67(6)	7(6)
C(16)	316(8)	222(6)	151(5)	-18(5)	9(6)	-32(6)
C(17)	223(7)	213(5)	154(5)	14(4)	-8(6)	-20(6)
C(18)	140(6)	155(5)	155(5)	8(4)	2(5)	-12(4)
C(19)	167(7)	350(7)	189(5)	-53(5)	21(5)	27(6)
C(20)	248(10)	717(13)	368(9)	4(9)	16(8)	224(9)
C(21)	243(9)	482(9)	323(7)	-132(7)	110(8)	-140(8)
C(22)	281(8)	163(5)	211(6)	-26(4)	50(6)	-3(5)
C(23)	308(10)	305(7)	343(7)	-31(6)	100(8)	-106(7)
C(24)	536(12)	181(6)	259(7)	32(5)	47(7)	20(7)
C(25)	156(7)	211(6)	187(5)	28(4)	-33(5)	-1(5)
C(26)	228(8)	243(6)	358(7)	14(5)	-83(7)	67(6)
C(27)	169(7)	310(8)	402(8)	106(7)	-27(7)	-25(6)
C(28)	184(7)	167(5)	195(5)	32(4)	0(5)	-4(5)
C(29)	279(9)	291(7)	204(6)	81(5)	21(6)	-28(7)
C(30)	168(7)	241(6)	273(6)	17(5)	15(6)	-21(6)

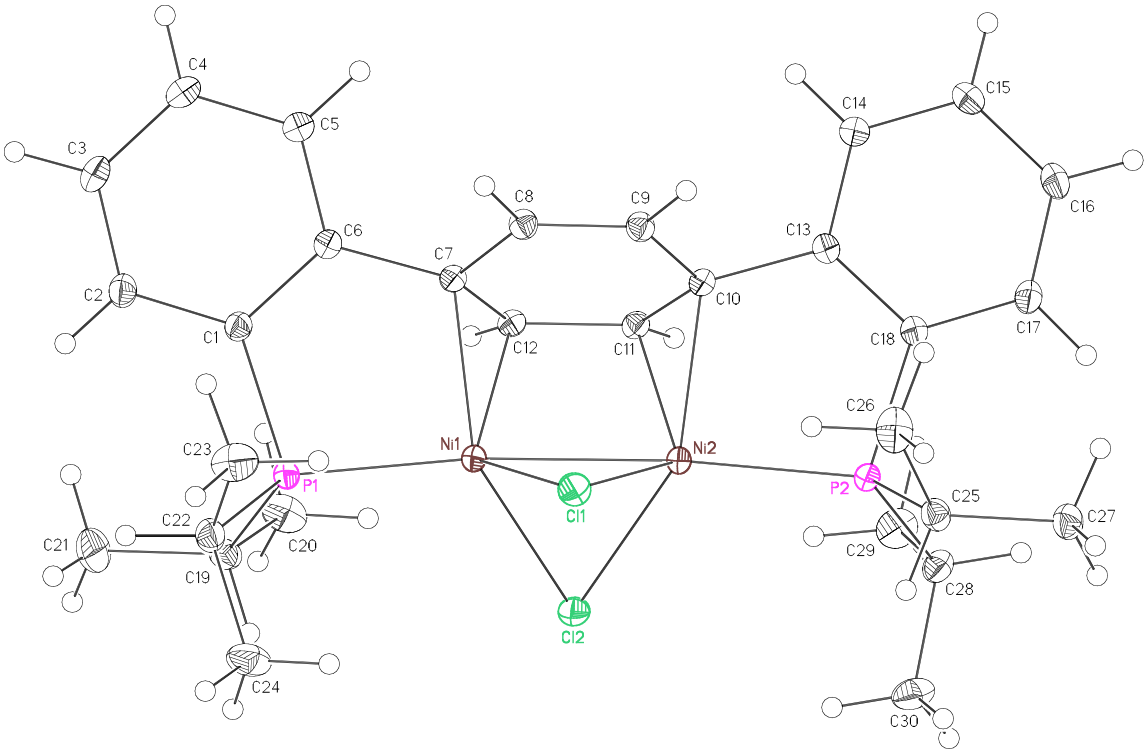

Figure 2. Structural drawing of **3** with 50% thermal probability ellipsoids.

Special refinement details for 3. Crystals were mounted on a glass fiber using Paratone oil then placed on the diffractometer under a nitrogen stream at 100K. Refinement of F^2 against ALL reflections. The weighted R-factor (*w*R) and goodness of fit (S) are based on F^2, conventional R-factors (R) are based on F, with F set to zero for negative F^2. The threshold expression of $F^2 > 2\sigma(F^2)$ is used only for calculating R-factors(gt) etc. and is not relevant to the choice of reflections for refinement. R-factors based on F^2 are statistically about twice as large as those based on F, and R-factors based on ALL data will be even larger. All esds (except the esd in the dihedral angle between two l.s. planes) are estimated using the full covariance matrix. The cell esds are taken into account individually in the estimation of esds in distances, angles and torsion angles; correlations between esds in cell parameters are only used when they are defined by crystal symmetry. An approximate (isotropic) treatment of cell esds is used for estimating esds involving l.s. planes.

Table 5. Atomic coordinates (x 10^4) and equivalent isotropic displacement parameters ($Å^2$x 10^3) for **3**. U(eq) is defined as the trace of the orthogonalized U^{ij} tensor.

	x	y	z	U_{eq}
Ni(1)	7467(1)	10973(1)	3403(1)	10(1)
Ni(2)	7112(1)	9568(1)	1996(1)	11(1)
Cl(1)	5248(1)	10664(1)	2439(1)	14(1)
Cl(2)	8442(1)	11110(1)	2049(1)	15(1)
P(1)	7956(1)	12355(1)	4608(1)	11(1)
P(2)	6815(1)	8368(1)	635(1)	11(1)
C(1)	7990(1)	11779(1)	5656(1)	12(1)
C(2)	8166(1)	12360(1)	6616(1)	15(1)
C(3)	8061(1)	11849(1)	7362(1)	15(1)
C(4)	7759(1)	10754(1)	7152(1)	15(1)
C(5)	7558(1)	10172(1)	6198(1)	13(1)
C(6)	7679(1)	10671(1)	5438(1)	11(1)
C(7)	7411(1)	10021(1)	4415(1)	11(1)
C(8)	6155(1)	9312(1)	4130(1)	12(1)
C(9)	5962(1)	8517(1)	3321(1)	12(1)
C(10)	7015(1)	8320(1)	2703(1)	11(1)
C(11)	8333(1)	8926(1)	3022(1)	11(1)
C(12)	8533(1)	9773(1)	3876(1)	11(1)
C(13)	6935(1)	7242(1)	2032(1)	12(1)
C(14)	6879(1)	6330(1)	2408(1)	15(1)
C(15)	6854(1)	5324(1)	1805(1)	18(1)
C(16)	6896(1)	5214(1)	825(1)	18(1)
C(17)	6930(1)	6110(1)	441(1)	15(1)
C(18)	6922(1)	7128(1)	1040(1)	12(1)
C(19)	9660(1)	13109(1)	4742(1)	16(1)
C(20)	10823(1)	12331(1)	4617(1)	22(1)
C(21)	10063(1)	13979(1)	5668(1)	26(1)
C(22)	6662(1)	13388(1)	4744(1)	16(1)
C(23)	5249(1)	12900(1)	4844(1)	23(1)
C(24)	6502(1)	13894(1)	3868(1)	22(1)
C(25)	5055(1)	8280(1)	-119(1)	14(1)
C(26)	3930(1)	8162(1)	499(1)	21(1)
C(27)	4827(1)	7411(1)	-1052(1)	17(1)
C(28)	8102(1)	8289(1)	-191(1)	14(1)
C(29)	9570(1)	8207(1)	361(1)	20(1)
C(30)	8052(1)	9252(1)	-649(1)	20(1)
C(41)	2970(1)	4650(1)	2426(1)	32(1)
C(42)	2463(1)	3780(1)	2712(1)	32(1)
C(43)	1069(1)	3414(1)	2420(1)	33(1)
C(44)	185(1)	3930(1)	1845(1)	40(1)
C(45)	683(1)	4798(1)	1559(1)	42(1)
C(46)	2081(1)	5157(1)	1844(1)	37(1)

Table 6. Anisotropic displacement parameters ($Å^2 x\ 10^4$) for **3**. The anisotropic displacement factor exponent takes the form: $-2\pi^2[\ h^2 a^{*2} U^{11} + ... + 2\ h\ k\ a^*\ b^*\ U^{12}\ ]$

	U^{11}	U^{22}	U^{33}	U^{23}	U^{13}	U^{12}
Ni(1)	127(1)	92(1)	84(1)	13(1)	7(1)	-2(1)
Ni(2)	131(1)	92(1)	86(1)	11(1)	14(1)	-4(1)
Cl(1)	130(1)	148(1)	148(1)	38(1)	-9(1)	18(1)
Cl(2)	194(1)	143(1)	130(1)	37(1)	40(1)	-34(1)
P(1)	141(1)	93(1)	96(1)	16(1)	4(1)	0(1)
P(2)	122(1)	105(1)	88(1)	15(1)	16(1)	-1(1)
C(1)	131(3)	117(2)	103(3)	19(2)	6(2)	12(2)
C(2)	172(3)	137(2)	118(3)	5(2)	3(3)	5(2)
C(3)	152(3)	192(3)	98(3)	12(2)	9(2)	20(2)
C(4)	139(3)	195(3)	117(3)	54(2)	27(2)	23(2)
C(5)	137(3)	141(2)	125(3)	39(2)	24(2)	10(2)
C(6)	99(3)	119(2)	104(3)	22(2)	15(2)	15(2)
C(7)	119(3)	103(2)	99(3)	23(2)	20(2)	11(2)
C(8)	116(3)	123(2)	124(3)	17(2)	39(2)	8(2)
C(9)	117(3)	121(2)	121(3)	19(2)	23(2)	-6(2)
C(10)	128(3)	106(2)	93(3)	19(2)	22(2)	7(2)
C(11)	113(3)	117(2)	100(3)	25(2)	24(2)	13(2)
C(12)	109(3)	116(2)	99(3)	29(2)	14(2)	9(2)
C(13)	118(3)	105(2)	119(3)	15(2)	16(2)	3(2)
C(14)	201(3)	122(2)	127(3)	32(2)	24(3)	1(2)
C(15)	242(4)	110(2)	174(4)	33(2)	20(3)	3(2)
C(16)	243(4)	109(2)	166(4)	-1(2)	22(3)	14(2)
C(17)	201(3)	134(2)	114(3)	5(2)	23(3)	20(2)
C(18)	134(3)	107(2)	116(3)	15(2)	21(2)	8(2)
C(19)	171(3)	136(2)	161(4)	42(2)	0(3)	-29(2)
C(20)	156(3)	212(3)	298(5)	91(3)	13(3)	-2(3)
C(21)	276(4)	210(3)	228(5)	-13(3)	-14(3)	-101(3)
C(22)	196(3)	126(2)	136(3)	16(2)	0(3)	32(2)
C(23)	209(4)	272(4)	266(5)	114(3)	94(3)	79(3)
C(24)	202(4)	196(3)	259(4)	119(3)	-21(3)	0(3)
C(25)	136(3)	126(2)	141(3)	18(2)	1(2)	1(2)
C(26)	141(3)	247(3)	226(4)	-5(3)	47(3)	-16(3)
C(27)	184(3)	154(3)	143(4)	12(2)	-13(3)	-11(2)
C(28)	137(3)	175(3)	114(3)	24(2)	27(2)	-7(2)
C(29)	138(3)	259(3)	214(4)	64(3)	24(3)	13(3)
C(30)	189(4)	262(3)	181(4)	107(3)	30(3)	-22(3)
C(41)	283(5)	365(5)	272(5)	-37(4)	66(4)	-9(4)
C(42)	308(5)	414(5)	231(5)	45(4)	33(4)	58(4)
C(43)	346(5)	352(5)	277(5)	-34(4)	129(4)	-5(4)
C(44)	265(5)	486(6)	353(6)	-82(5)	38(4)	60(4)
C(45)	440(6)	473(6)	311(6)	8(5)	26(5)	242(5)
C(46)	561(7)	261(4)	302(6)	-6(4)	201(5)	94(4)

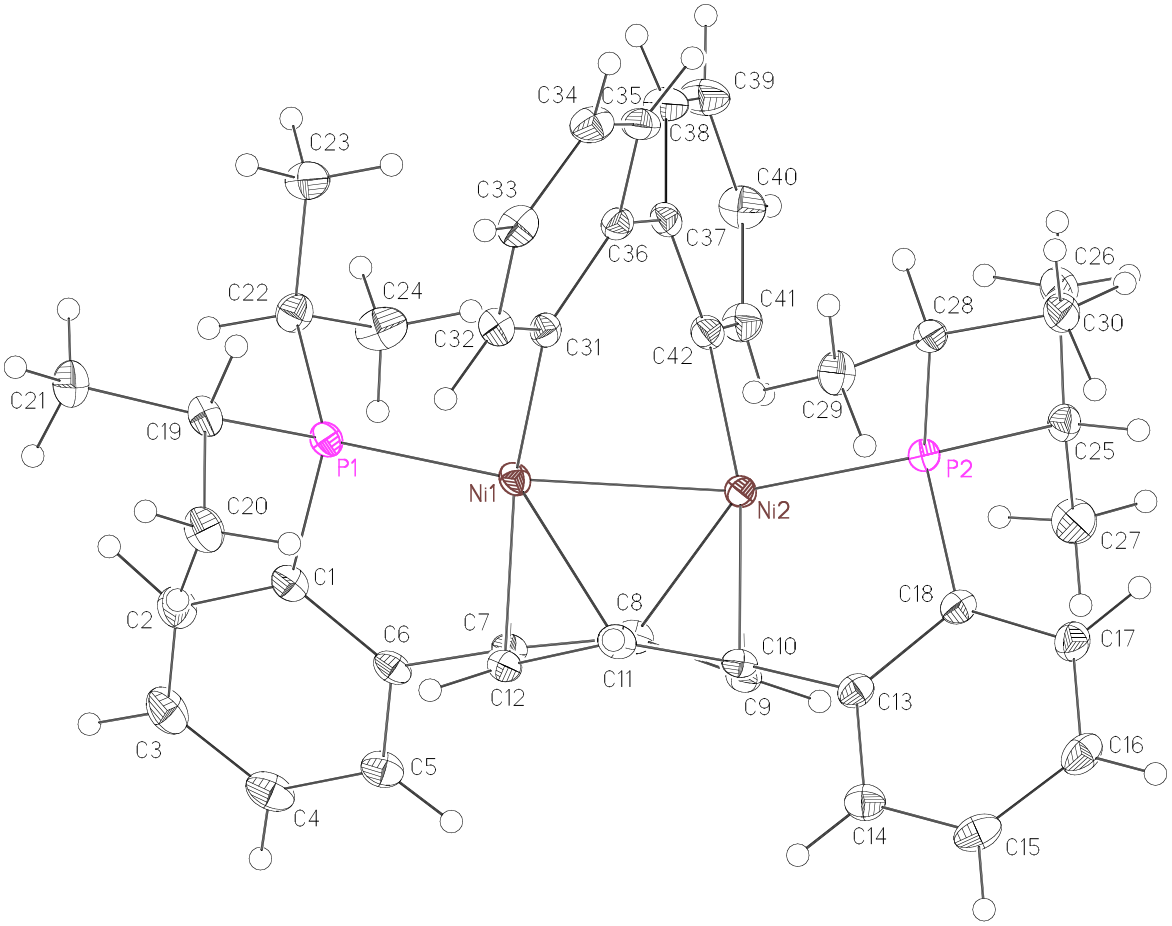

Figure 3. Structural drawing of **4** with 50% thermal probability ellipsoids.

Special refinement details for 4. Crystals were mounted on a glass fiber using Paratone oil then placed on the diffractometer under a nitrogen stream at 100K. The central ring of the ligand (C7-C12) is distorted from planarity by as much as 0.17A as shown below;

Least-squares planes (x,y,z in crystal coordinates) and deviations from them

(* indicates atom used to define plane)

7.4146 (0.0035) x + 3.1875 (0.0051) y - 11.3528 (0.0038) z = 0.9319 (0.0017)

* 0.0076 (0.0007) C7

* -0.1722 (0.0007) C8

* 0.1656 (0.0007) C9

* 0.0048 (0.0007) C10

* -0.1693 (0.0007) C11

* 0.1635 (0.0007) C12

Rms deviation of fitted atoms = 0.1370

Refinement of F^2 against ALL reflections. All esds (except the esd in the dihedral angle between two l.s. planes) are estimated using the full covariance matrix. The cell esds are taken into account individually in the estimation of esds in distances, angles and torsion angles; correlations between esds in cell parameters are only used when they are defined by crystal symmetry. An approximate (isotropic) treatment of cell esds is used for estimating esds involving l.s. planes.

Table 7. Atomic coordinates (x 10^4) and equivalent isotropic displacement parameters (Å^{2}x 10^3) for **4**. U(eq) is defined as the trace of the orthogonalized U^{ij} tensor.

	x	y	z	U_{eq}
Ni(1)	1249(1)	2324(1)	2231(1)	12(1)
Ni(2)	2988(1)	2346(1)	3357(1)	12(1)
P(1)	94(1)	3187(1)	1980(1)	13(1)
P(2)	3519(1)	1116(1)	3797(1)	12(1)
C(1)	1243(1)	4473(1)	1728(1)	15(1)
C(2)	986(1)	5341(1)	1513(1)	19(1)
C(3)	1983(1)	6366(1)	1479(1)	21(1)
C(4)	3268(1)	6562(1)	1672(1)	20(1)
C(5)	3539(1)	5707(1)	1880(1)	17(1)
C(6)	2538(1)	4655(1)	1891(1)	14(1)
C(7)	2808(1)	3695(1)	2044(1)	13(1)
C(8)	3778(1)	3918(1)	2898(1)	14(1)
C(9)	4439(1)	3227(1)	2838(1)	14(1)
C(10)	3733(1)	2037(1)	2185(1)	13(1)
C(11)	2542(1)	1698(1)	1465(1)	14(1)
C(12)	2304(1)	2597(1)	1269(1)	13(1)
C(13)	4312(1)	1214(1)	2149(1)	14(1)
C(14)	4813(1)	904(1)	1375(1)	17(1)
C(15)	5462(1)	240(1)	1399(1)	19(1)
C(16)	5638(1)	-100(1)	2193(1)	19(1)
C(17)	5113(1)	173(1)	2950(1)	18(1)
C(18)	4416(1)	808(1)	2926(1)	14(1)
C(19)	-1391(1)	2266(1)	931(1)	16(1)
C(20)	-1027(1)	1819(1)	12(1)	20(1)
C(21)	-2269(1)	2818(1)	740(1)	21(1)
C(22)	-444(1)	3905(1)	2964(1)	16(1)
C(23)	-1520(1)	2981(1)	3240(1)	21(1)
C(24)	726(1)	4778(1)	3848(1)	23(1)
C(25)	4630(1)	1607(1)	5009(1)	15(1)
C(26)	3915(1)	1680(1)	5798(1)	20(1)
C(27)	5835(1)	2803(1)	5207(1)	23(1)
C(28)	2170(1)	-379(1)	3627(1)	14(1)
C(29)	1364(1)	-986(1)	2563(1)	19(1)
C(30)	2587(1)	-1209(1)	3957(1)	18(1)
C(31)	-16(1)	951(1)	2431(1)	13(1)
C(32)	-898(1)	-41(1)	1602(1)	16(1)
C(33)	-1816(1)	-1104(1)	1663(1)	17(1)

C(34)	-1866(1)	-1208(1)	2569(1)	18(1)
C(35)	-1015(1)	-241(1)	3402(1)	16(1)
C(36)	-107(1)	838(1)	3349(1)	13(1)
C(37)	763(1)	1879(1)	4246(1)	13(1)
C(38)	274(1)	2117(1)	5049(1)	18(1)
C(39)	1033(1)	3119(1)	5883(1)	22(1)
C(40)	2295(1)	3906(1)	5918(1)	21(1)
C(41)	2788(1)	3680(1)	5124(1)	17(1)
C(42)	2059(1)	2654(1)	4278(1)	14(1)
C(51)	2220(2)	4310(2)	8679(1)	46(1)
C(52)	3684(1)	5121(1)	9142(1)	32(1)
C(53)	4295(1)	4576(1)	9706(1)	25(1)

Table 8. Anisotropic displacement parameters ($Å^2 x\ 10^4$) for **4**. The anisotropic displacement factor exponent takes the form: $-2\pi^2[\ h^2 a^{*2} U^{11} + ... + 2\ h\ k\ a^*\ b^*\ U^{12}\ ]$

	U^{11}	U^{22}	U^{33}	U^{23}	U^{13}	U^{12}
Ni(1)	125(1)	100(1)	131(1)	55(1)	30(1)	46(1)
Ni(2)	128(1)	122(1)	118(1)	49(1)	41(1)	66(1)
P(1)	142(1)	114(1)	123(1)	44(1)	30(1)	59(1)
P(2)	122(1)	134(1)	130(1)	57(1)	40(1)	66(1)
C(1)	188(5)	122(5)	133(5)	44(4)	51(4)	78(4)
C(2)	238(5)	177(6)	214(6)	88(5)	77(4)	125(5)
C(3)	319(6)	152(6)	212(6)	85(5)	76(5)	136(5)
C(4)	271(6)	117(5)	197(6)	66(5)	91(4)	64(5)
C(5)	200(5)	134(5)	172(5)	55(4)	70(4)	67(4)
C(6)	191(5)	112(5)	103(4)	38(4)	52(4)	67(4)
C(7)	144(4)	116(5)	130(5)	53(4)	59(4)	60(4)
C(8)	153(4)	104(5)	130(5)	29(4)	43(4)	44(4)
C(9)	136(4)	139(5)	140(5)	60(4)	43(4)	52(4)
C(10)	134(4)	137(5)	124(5)	57(4)	61(3)	62(4)
C(11)	169(5)	108(5)	120(5)	23(4)	47(4)	60(4)
C(12)	137(4)	135(5)	123(5)	53(4)	42(4)	59(4)
C(13)	121(4)	120(5)	158(5)	37(4)	40(4)	51(4)
C(14)	175(5)	171(6)	159(5)	49(4)	56(4)	74(4)
C(15)	165(5)	163(6)	209(6)	14(5)	79(4)	69(4)
C(16)	156(5)	150(6)	283(6)	63(5)	73(4)	87(4)
C(17)	162(5)	169(6)	226(6)	92(5)	57(4)	92(4)
C(18)	130(4)	130(5)	164(5)	46(4)	48(4)	63(4)
C(19)	176(5)	140(5)	145(5)	55(4)	13(4)	64(4)
C(20)	236(5)	177(6)	151(5)	40(5)	17(4)	92(5)
C(21)	209(5)	237(7)	197(6)	76(5)	19(4)	121(5)
C(22)	170(5)	161(5)	166(5)	44(4)	47(4)	90(4)
C(23)	189(5)	220(6)	196(6)	71(5)	72(4)	84(5)
C(24)	204(5)	220(6)	180(6)	-7(5)	47(4)	66(5)
C(25)	136(4)	164(5)	147(5)	56(4)	21(4)	71(4)
C(26)	210(5)	250(7)	152(5)	78(5)	43(4)	120(5)
C(27)	183(5)	207(6)	221(6)	65(5)	15(5)	43(5)
C(28)	134(4)	149(5)	160(5)	69(4)	56(4)	77(4)

C(29)	189(5)	167(6)	187(5)	43(5)	25(4)	92(5)
C(30)	172(5)	163(6)	235(6)	106(5)	59(4)	82(4)
C(31)	135(4)	109(5)	151(5)	53(4)	42(4)	70(4)
C(32)	169(5)	148(5)	143(5)	53(4)	34(4)	73(4)
C(33)	149(5)	122(5)	196(5)	18(4)	24(4)	47(4)
C(34)	165(5)	113(5)	257(6)	74(5)	87(4)	48(4)
C(35)	170(5)	158(5)	180(5)	84(4)	89(4)	78(4)
C(36)	127(4)	131(5)	147(5)	53(4)	49(4)	72(4)
C(37)	153(4)	127(5)	138(5)	63(4)	43(4)	75(4)
C(38)	178(5)	190(6)	168(5)	64(5)	76(4)	62(4)
C(39)	244(6)	247(7)	158(5)	53(5)	100(4)	98(5)
C(40)	220(5)	183(6)	144(5)	11(5)	31(4)	67(5)
C(41)	155(5)	164(6)	168(5)	42(4)	34(4)	57(4)
C(42)	152(4)	139(5)	138(5)	60(4)	44(4)	74(4)
C(51)	366(8)	349(9)	544(11)	-20(8)	-60(7)	219(7)
C(52)	309(7)	305(8)	358(8)	109(7)	67(6)	179(6)
C(53)	250(6)	229(7)	267(6)	76(6)	103(5)	121(5)

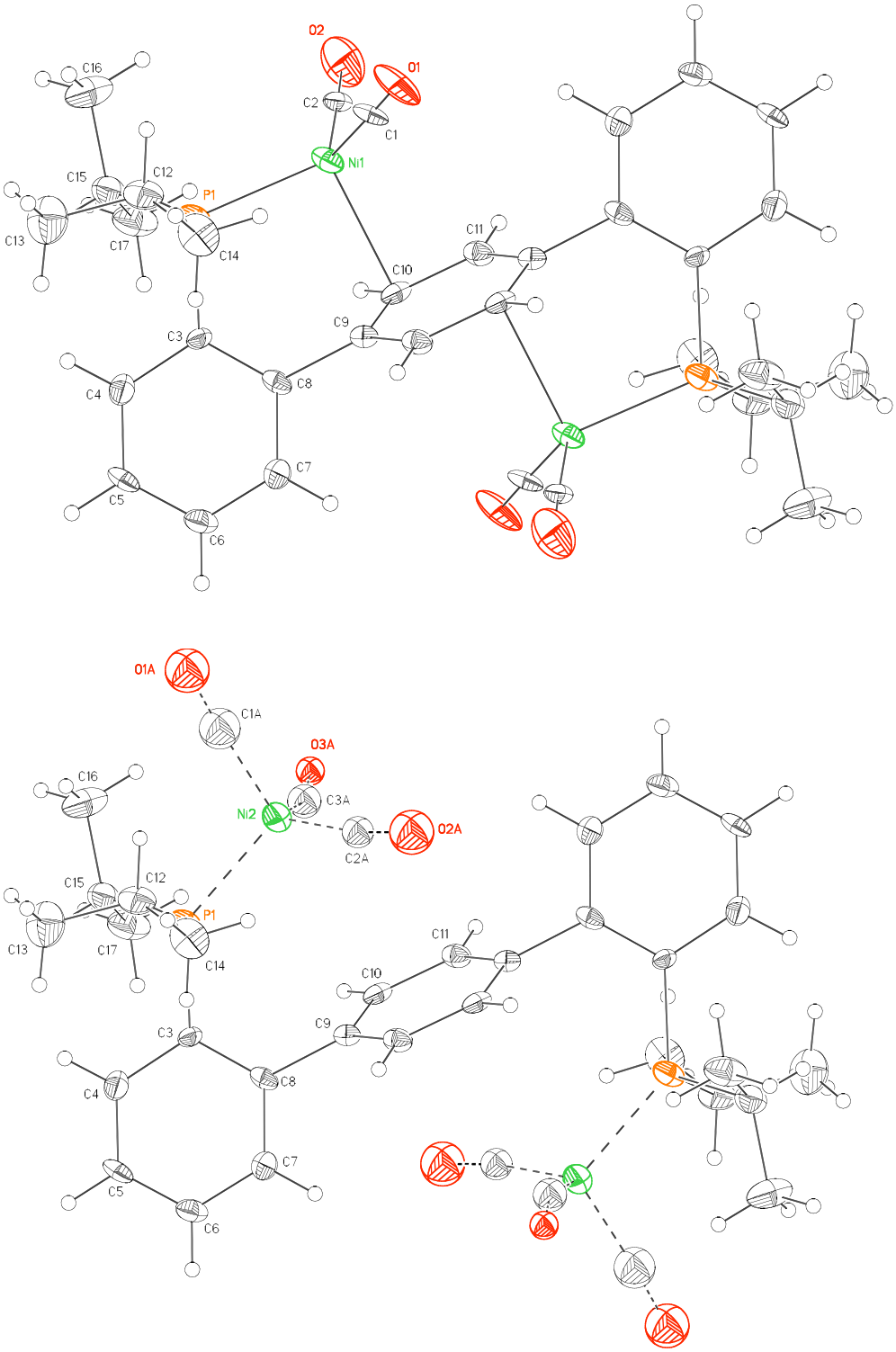

Figure 4. Structural drawings of species in **5** with 50% thermal probability ellipsoids. The mixed $[Ni(CO)_2Ni(CO)_3]$ species may also be present in the crystal (picture not shown).

Special refinement details for 5. Crystals were mounted on a glass fiber using Paratone

oil then placed on the diffractometer under a nitrogen stream at 100K.

The molecule sits at a center of symmetry AND is disordered between two distinctly different molecular formulas in an 80:20 ratio. The major component has two carbonyl ligands bonded to Ni and the Ni interacting with C10 of the central ring. In the minor component the Ni no longer interacts with C10 but now has three carbonyl ligands. The parameters of the minor component were refined with restraints to maintain somewhat reasonable geometry due to significant overlap of the atomic positions of C1 and C2A and of O2 and O3A, see figures 5and 6. Minor component parameters were then fixed for the final least-squares cycles.

Refinement of F^2 against ALL reflections. The weighted R-factor (*w*R) and goodness of fit (S) are based on F^2, conventional R-factors (R) are based on F, with F set to zero for negative F^2. The threshold expression of $F^2 > 2\delta(F^2)$ is used only for calculating R-factors(gt) etc. and is not relevant to the choice of reflections for refinement. R-factors based on F^2 are statistically about twice as large as those based on F, and R-factors based on ALL data will be even larger.

All esds (except the esd in the dihedral angle between two l.s. planes) are estimated using the full covariance matrix. The cell esds are taken into account individually in the estimation of esds in distances, angles and torsion angles; correlations between esds in cell parameters are only used when they are defined by crystal symmetry. An approximate (isotropic) treatment of cell esds is used for estimating esds involving l.s. planes.

Table 9. Atomic coordinates (x 10^4) and equivalent isotropic displacement parameters ($Å^2$x 10^3) for **5**. U(eq) is defined as the trace of the orthogonalized U^{ij} tensor.

	x	y	z	U_{eq}	Occ
Ni(1)	6188(1)	3933(1)	499(1)	21(1)	0.797(2)
P(1)	5925(2)	3584(1)	-1711(1)	23(1)	1
O(1)	9862(5)	4434(2)	1357(4)	41(1)	0.797(2)
O(2)	4847(5)	3277(2)	2559(4)	46(1)	0.797(2)
C(1)	8419(8)	4240(2)	1020(5)	29(2)	0.797(2)
C(2)	5328(7)	3546(2)	1731(5)	20(1)	0.797(2)
Ni(2)	7385	3680	577	25	0.20
O(1A)	10827	2990	983	50	0.20
O(2A)	9362	4711	1277	49	0.20
O(3A)	4705	3198	2297	26	0.20
C(1A)	9406	3249	819	45	0.20
C(2A)	8484	4313	963	18	0.20
C(3A)	5725	3436	1631	31	0.20
C(3)	4301(5)	3970(2)	-3049(4)	16(1)	1

C(4)	3512(5)	3758(1)	-4422(4)	22(1)	1
C(5)	2442(5)	4063(2)	-5478(4)	20(1)	1
C(6)	2181(5)	4586(2)	-5226(4)	22(1)	1
C(7)	2916(5)	4805(2)	-3908(4)	21(1)	1
C(8)	3947(5)	4493(2)	-2796(4)	16(1)	1
C(9)	4541(5)	4747(2)	-1352(4)	15(1)	1
C(10)	3850(5)	4560(1)	-158(4)	18(1)	1
C(11)	4315(5)	4806(1)	1189(4)	19(1)	1
C(12)	8105(5)	3572(2)	-2496(4)	27(1)	1
C(13)	8046(6)	3258(2)	-3879(4)	44(1)	1
C(14)	8767(6)	4132(1)	-2718(4)	34(1)	1
C(15)	5008(6)	2912(1)	-1953(4)	26(1)	1
C(16)	6365(6)	2526(2)	-1026(4)	43(1)	1
C(17)	3047(6)	2877(2)	-1577(4)	35(1)	1

Table 10. Anisotropic displacement parameters ($Å^2 x\ 10^4$) for **5**. The anisotropic displacement factor exponent takes the form: $-2\pi^2[\ h^2 a^{*2} U^{11} + ... + 2\ h\ k\ a^*\ b^*\ U^{12}\ ]$

	U^{11}	U^{22}	U^{33}	U^{23}	U^{13}	U^{12}
Ni(1)	167(4)	306(4)	144(3)	15(4)	-14(3)	14(4)
P(1)	227(7)	260(8)	167(6)	24(6)	-24(6)	-20(6)
O(1)	240(30)	710(30)	230(20)	-60(20)	-110(20)	-160(20)
O(2)	490(30)	660(30)	260(20)	-90(20)	100(20)	-110(20)
C(1)	330(40)	370(40)	120(30)	80(30)	-70(30)	40(30)
C(2)	250(40)	190(30)	120(30)	40(30)	-30(30)	130(30)
Ni(2)	280	310	140	10	-10	10
C(3)	200(20)	130(20)	140(20)	40(20)	31(19)	50(20)
C(4)	260(30)	180(30)	220(20)	-30(20)	60(20)	30(20)
C(5)	160(20)	300(30)	110(20)	10(20)	-36(19)	-30(20)
C(6)	190(30)	240(30)	200(20)	40(20)	-40(20)	-10(20)
C(7)	240(30)	160(30)	220(20)	-10(20)	40(20)	-10(20)
C(8)	130(20)	260(30)	90(20)	30(20)	41(19)	0(20)
C(9)	120(20)	160(30)	150(20)	34(19)	20(20)	5(19)
C(10)	130(20)	110(30)	270(30)	40(20)	-10(20)	10(20)
C(11)	170(30)	250(30)	150(20)	40(20)	50(20)	40(20)
C(12)	120(30)	390(30)	290(30)	50(20)	20(20)	30(20)
C(13)	350(30)	480(30)	520(30)	-80(30)	170(30)	-10(30)
C(14)	220(30)	490(30)	340(30)	-10(20)	130(20)	-80(20)
C(15)	300(30)	240(30)	220(20)	30(20)	0(20)	-10(20)
C(16)	390(30)	340(30)	520(30)	140(30)	0(30)	90(30)
C(17)	300(30)	340(30)	360(30)	110(20)	-60(20)	-80(20)

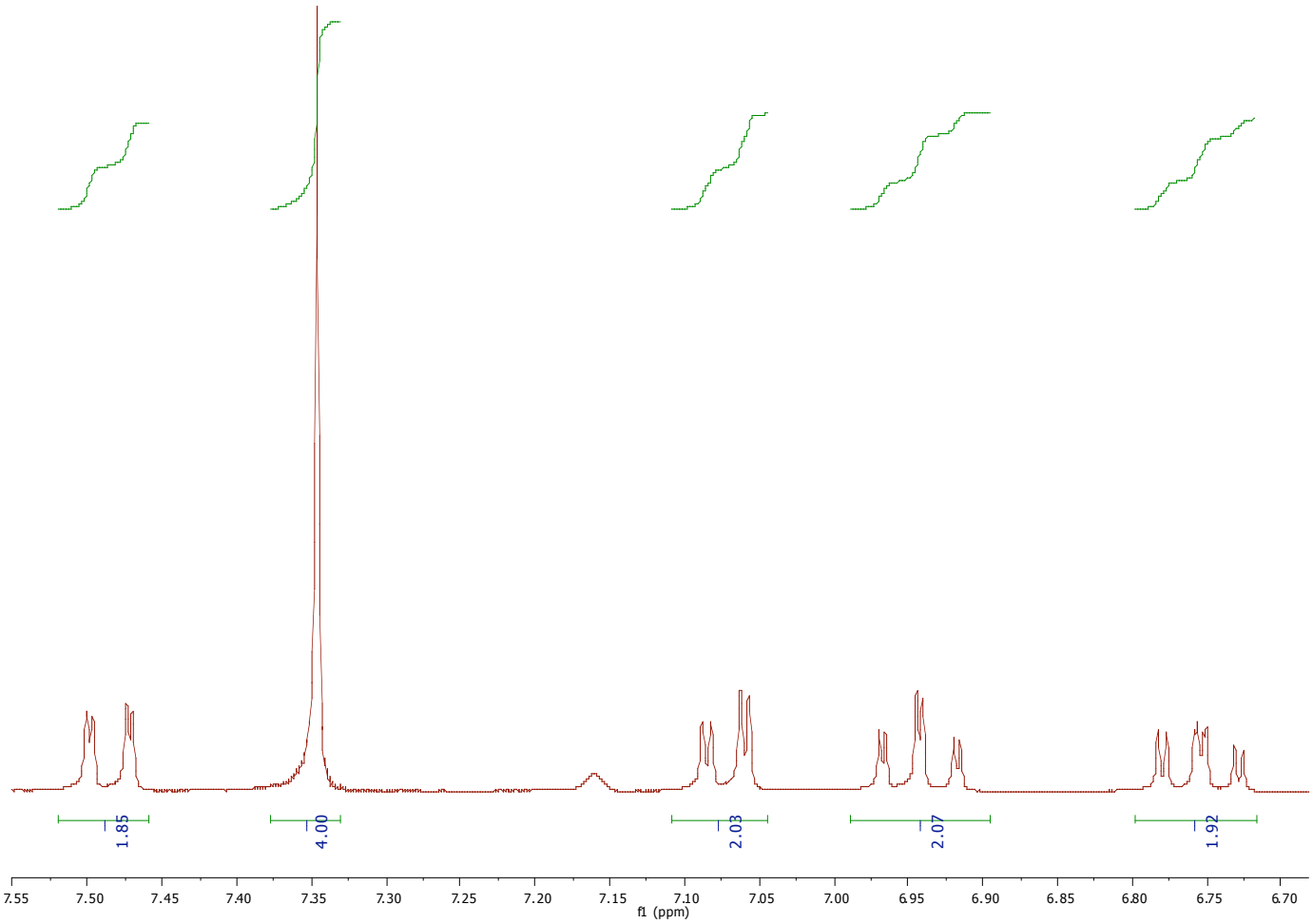

Figure 5. ^{1}H NMR spectrum of 1,4-bis(2-bromophenyl)-benzene in C_6D_6

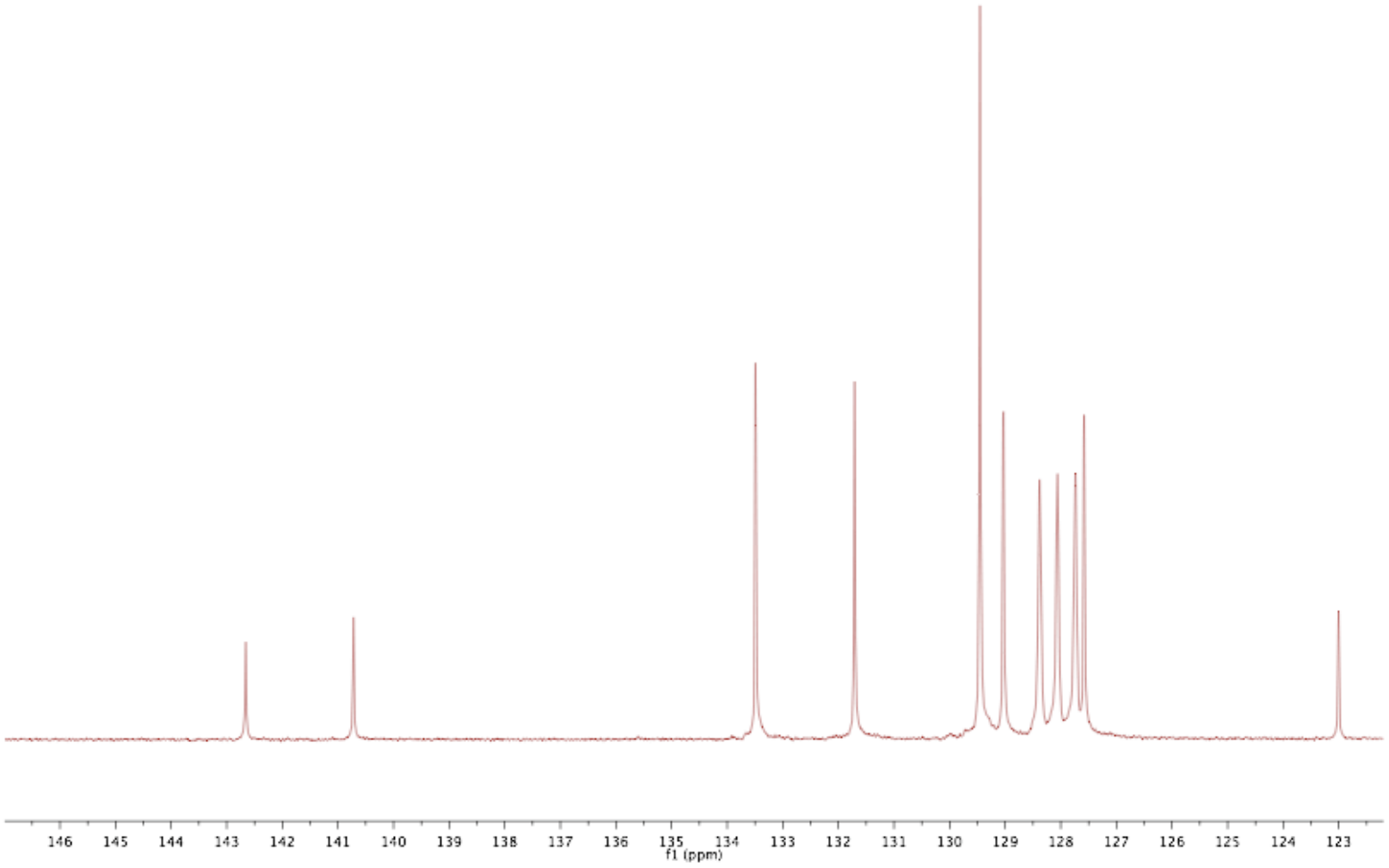

Figure 6. $^{13}C\{^{1}H\}$ NMR spectrum of 1,4-bis(2-bromophenyl)-benzene in C_6D_6

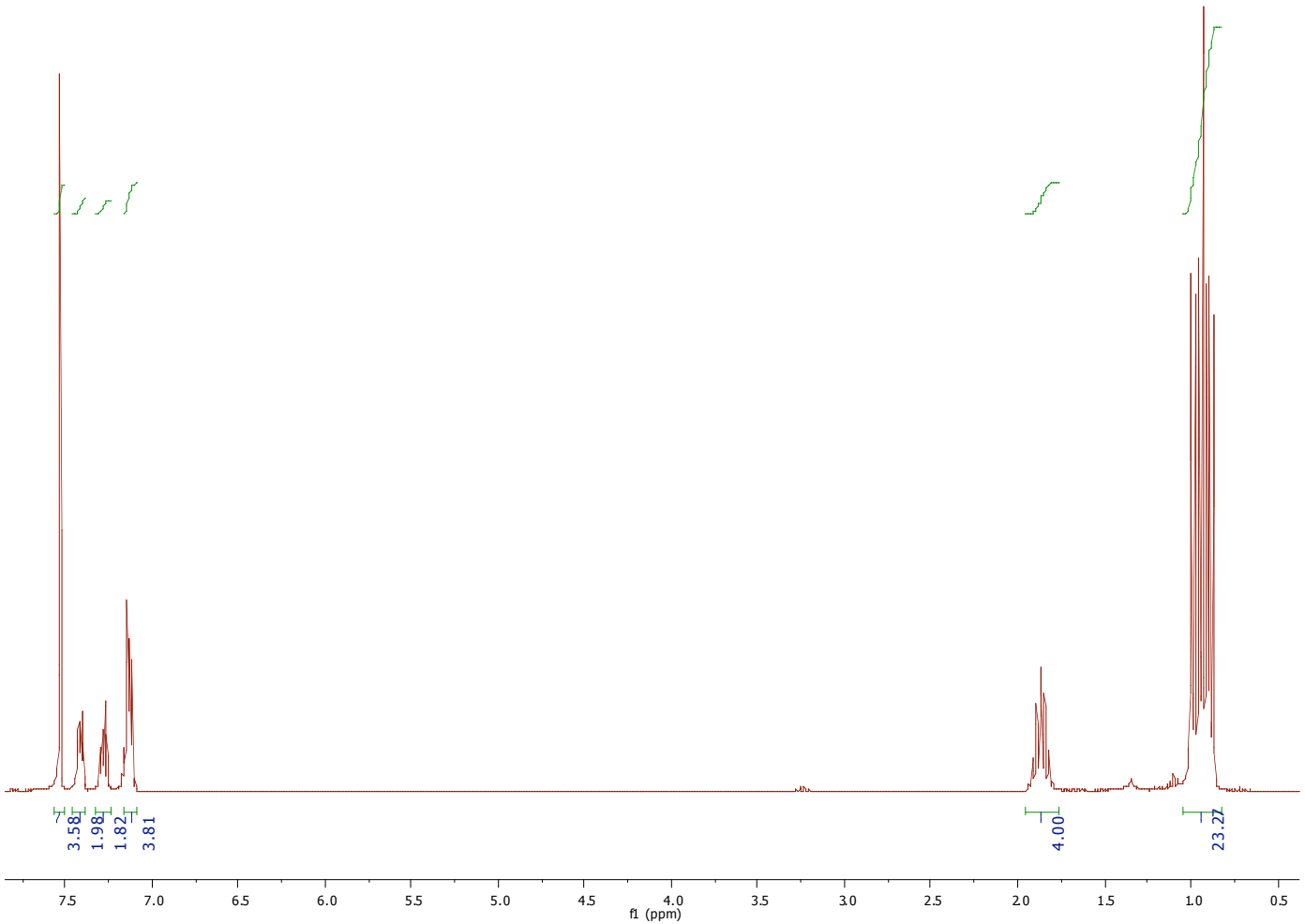

Figure 7. ^{1}H NMR spectrum of **1** in C_6D_6

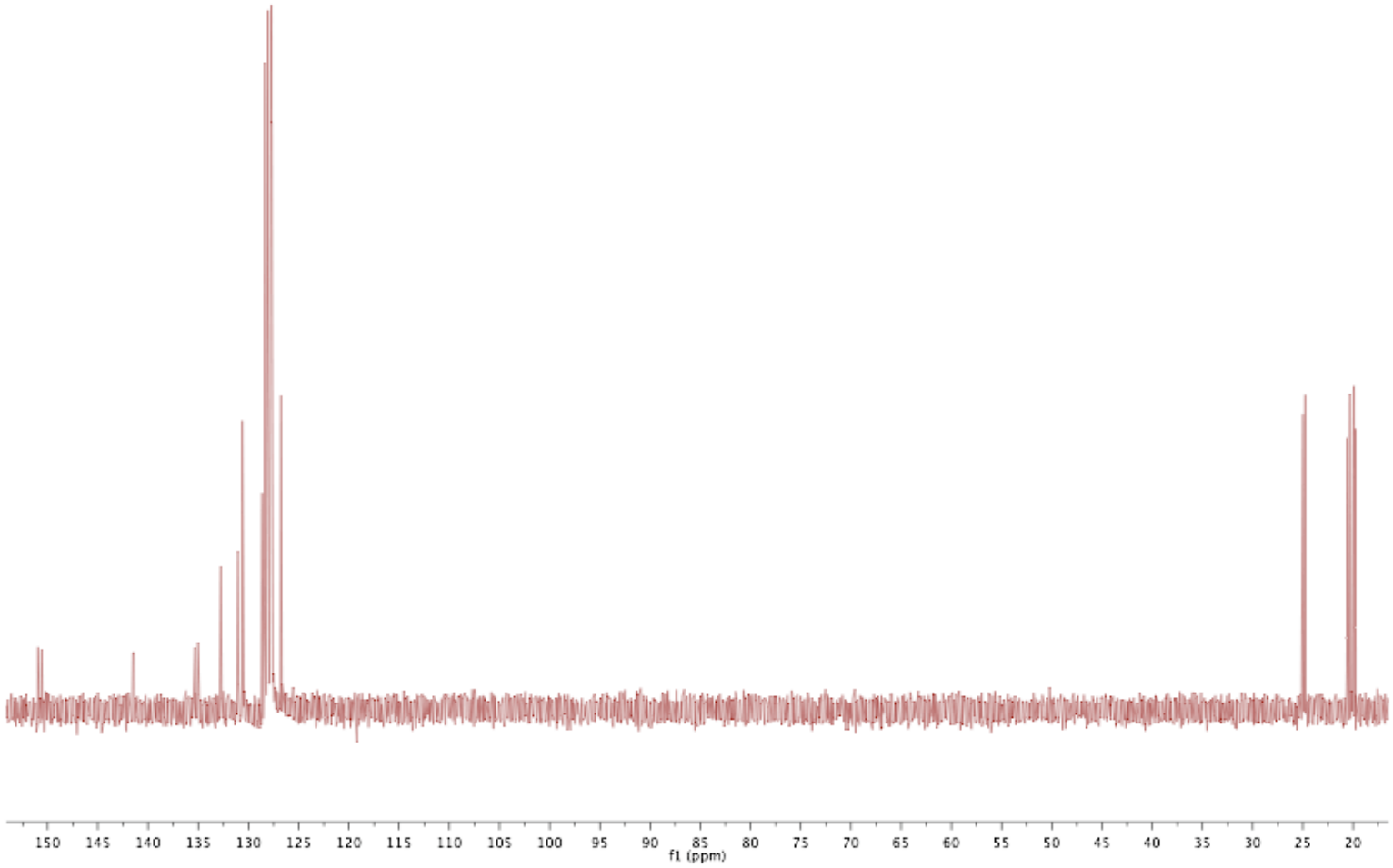

Figure 8. $^{13}C\{^{1}H\}$ NMR spectrum of **1** in C_6D_6

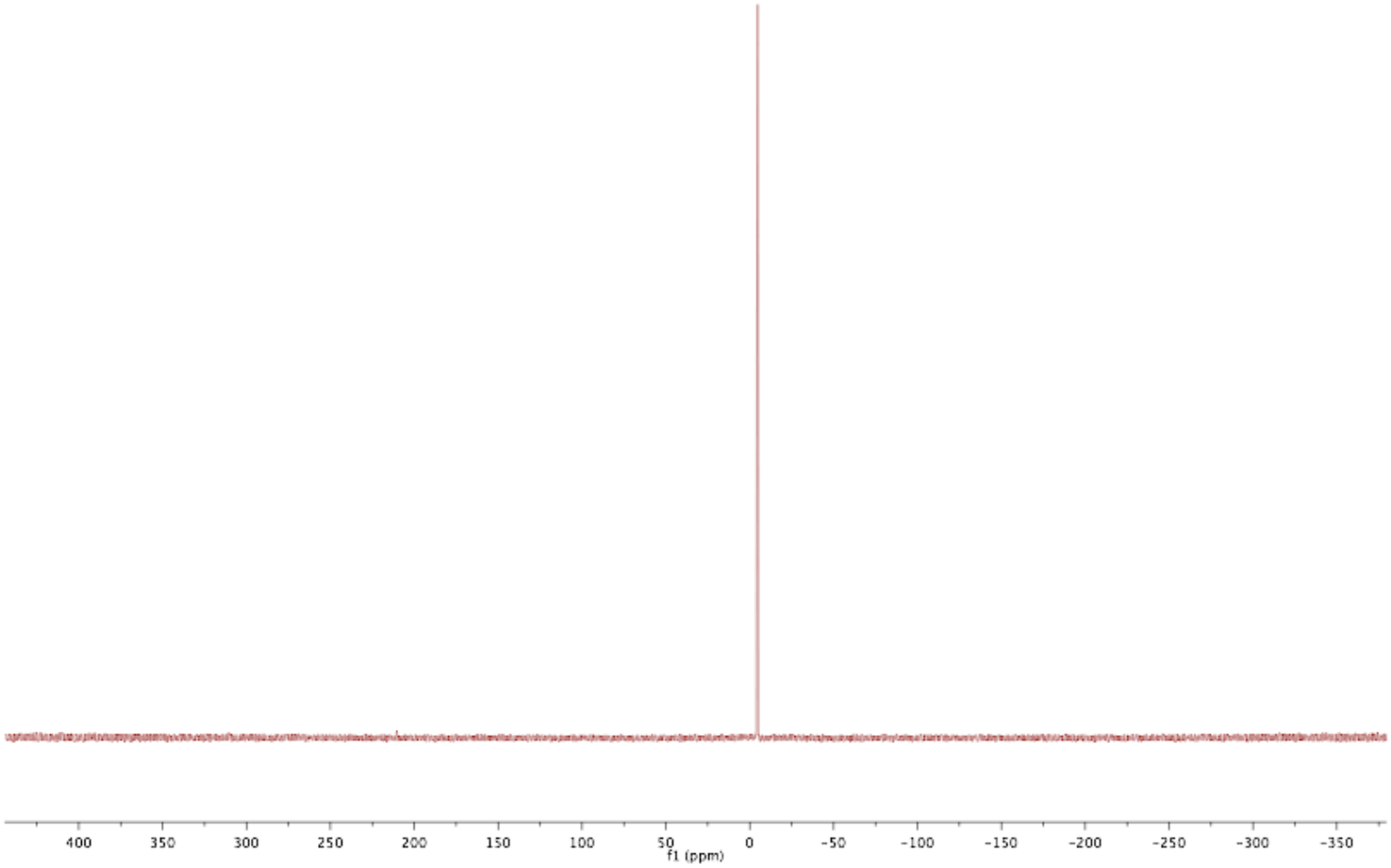

Figure 9. $^{31}P\{^{1}H\}$ NMR spectrum of **1** in C_6D_6

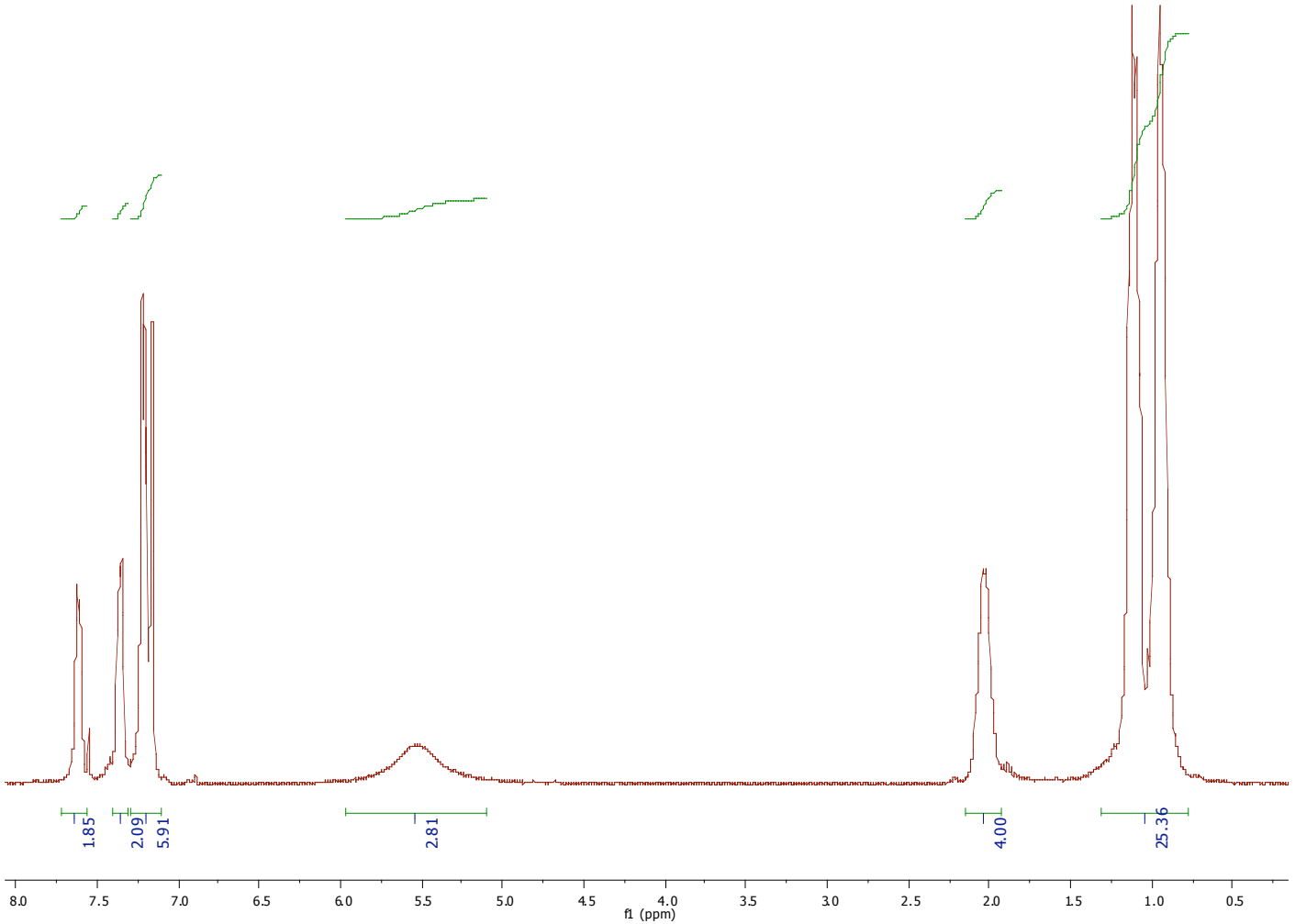

Figure 10. ^{1}H NMR spectrum of **2** in C_6D_6

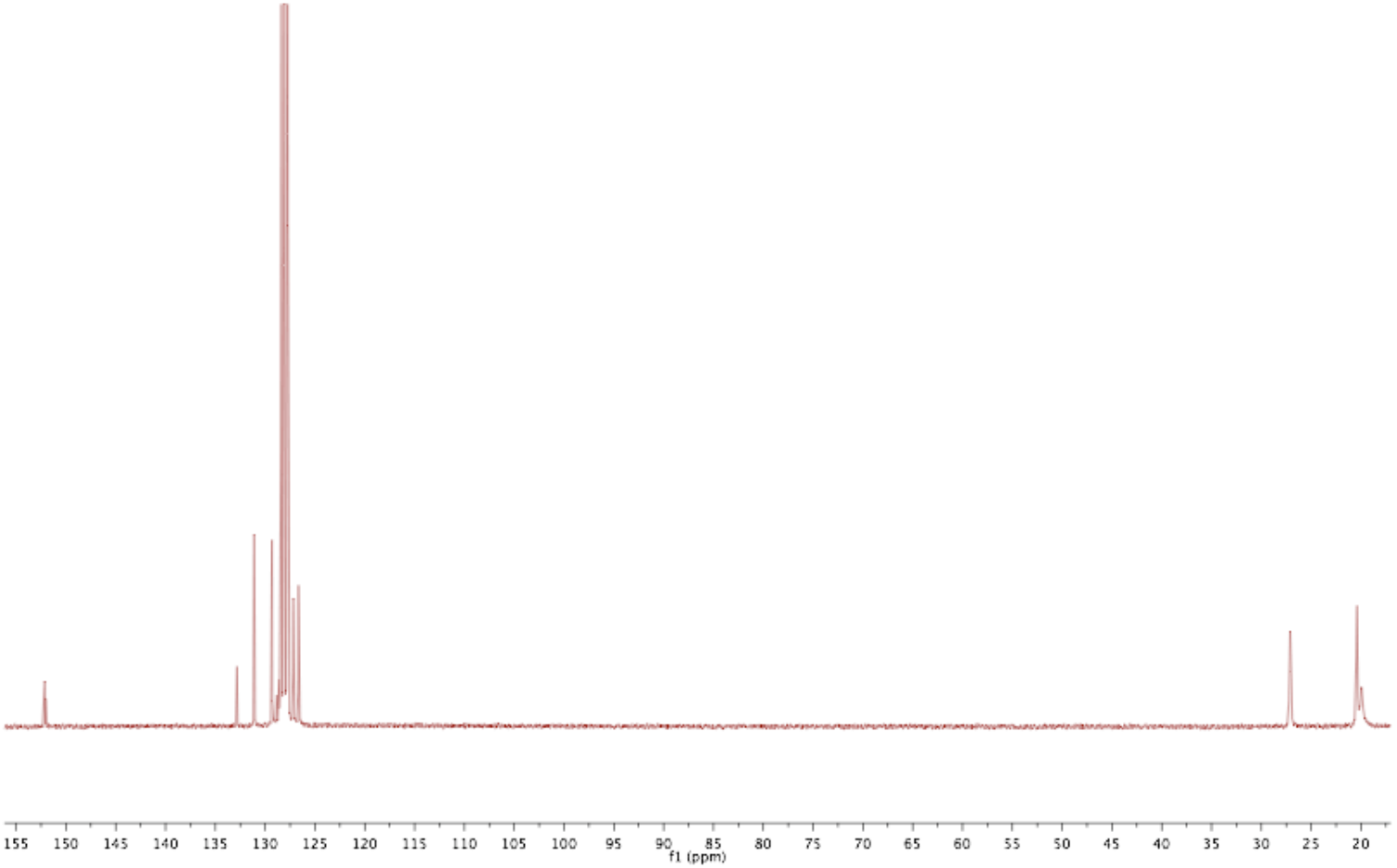

Figure 11. $^{13}C\{^{1}H\}$ NMR spectrum of **2** in C_6D_6

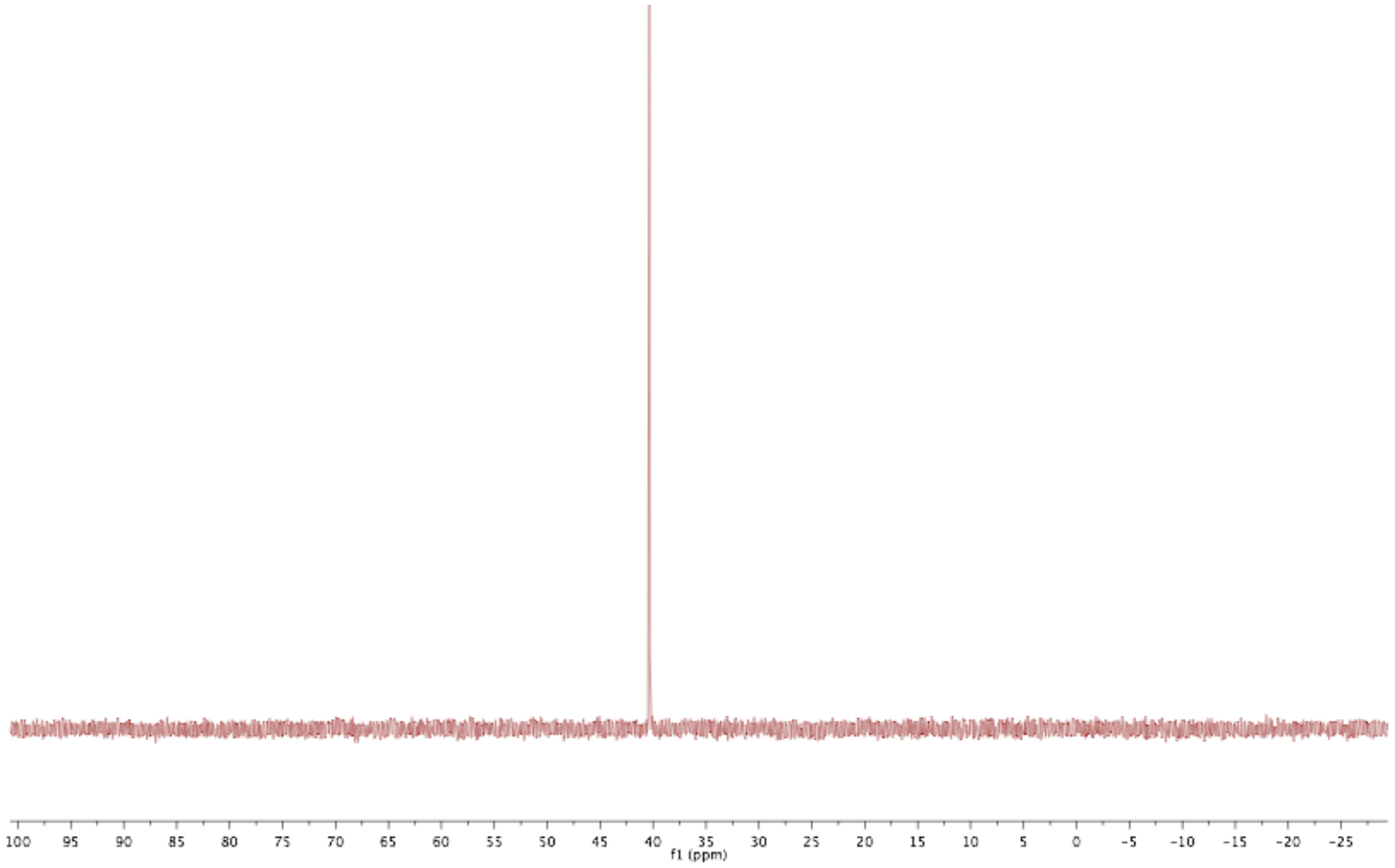

Figure 12. $^{31}P\{^{1}H\}$ NMR spectrum of **2** in C_6D_6

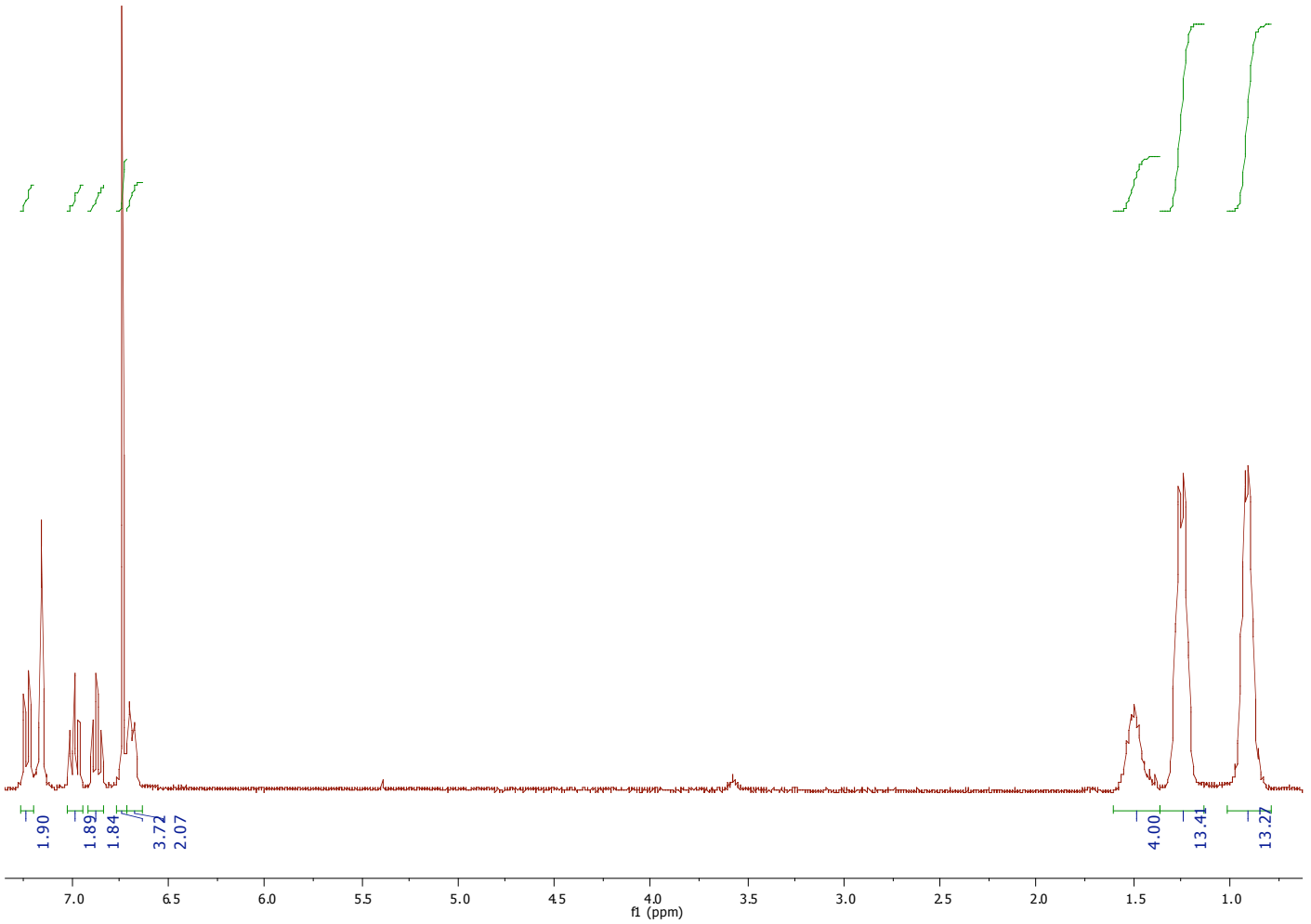

Figure 13. ^{1}H NMR spectrum of **3** in C_6D_6

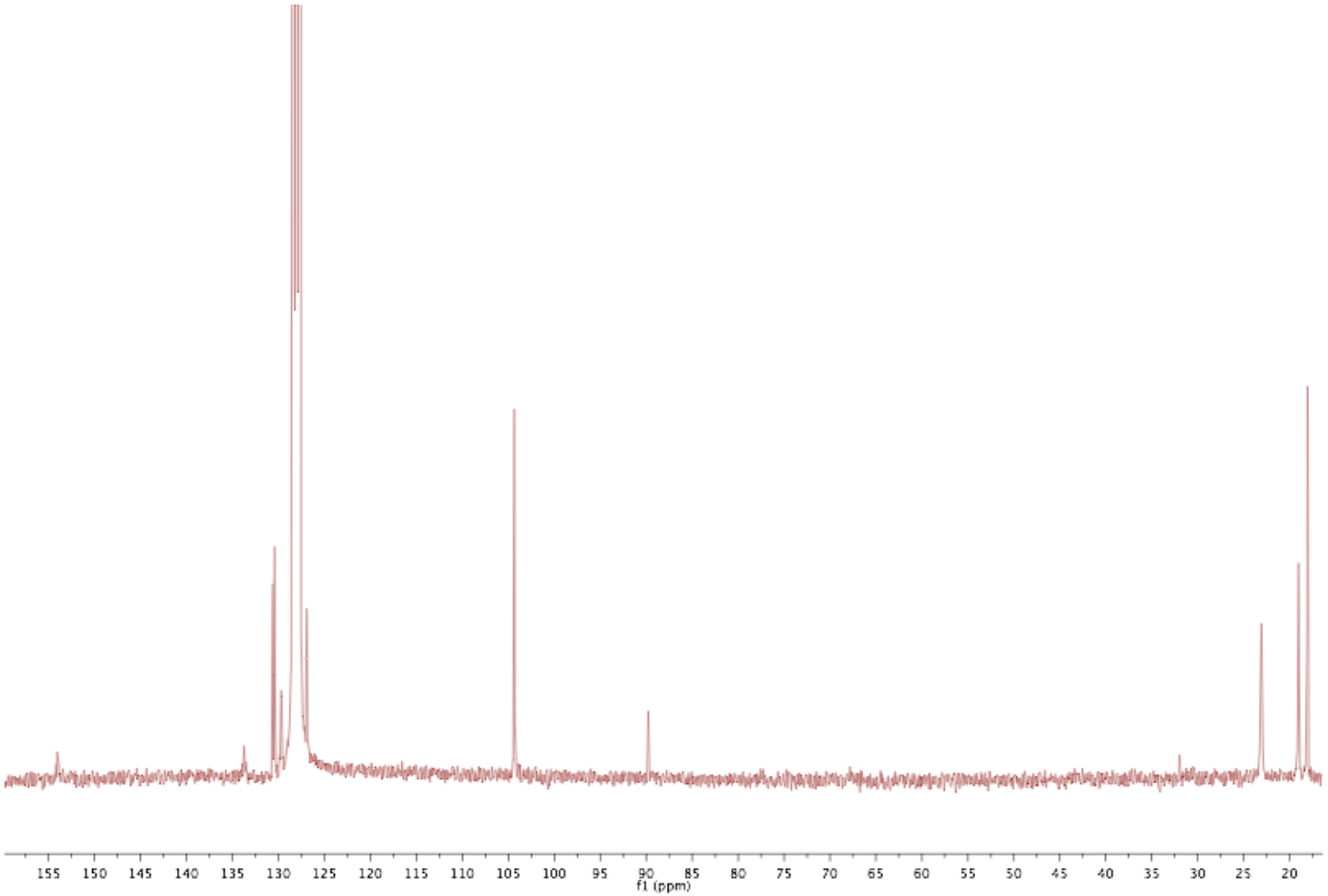

Figure 14. $^{13}C\{^{1}H\}$ NMR spectrum of **3** in C_6D_6

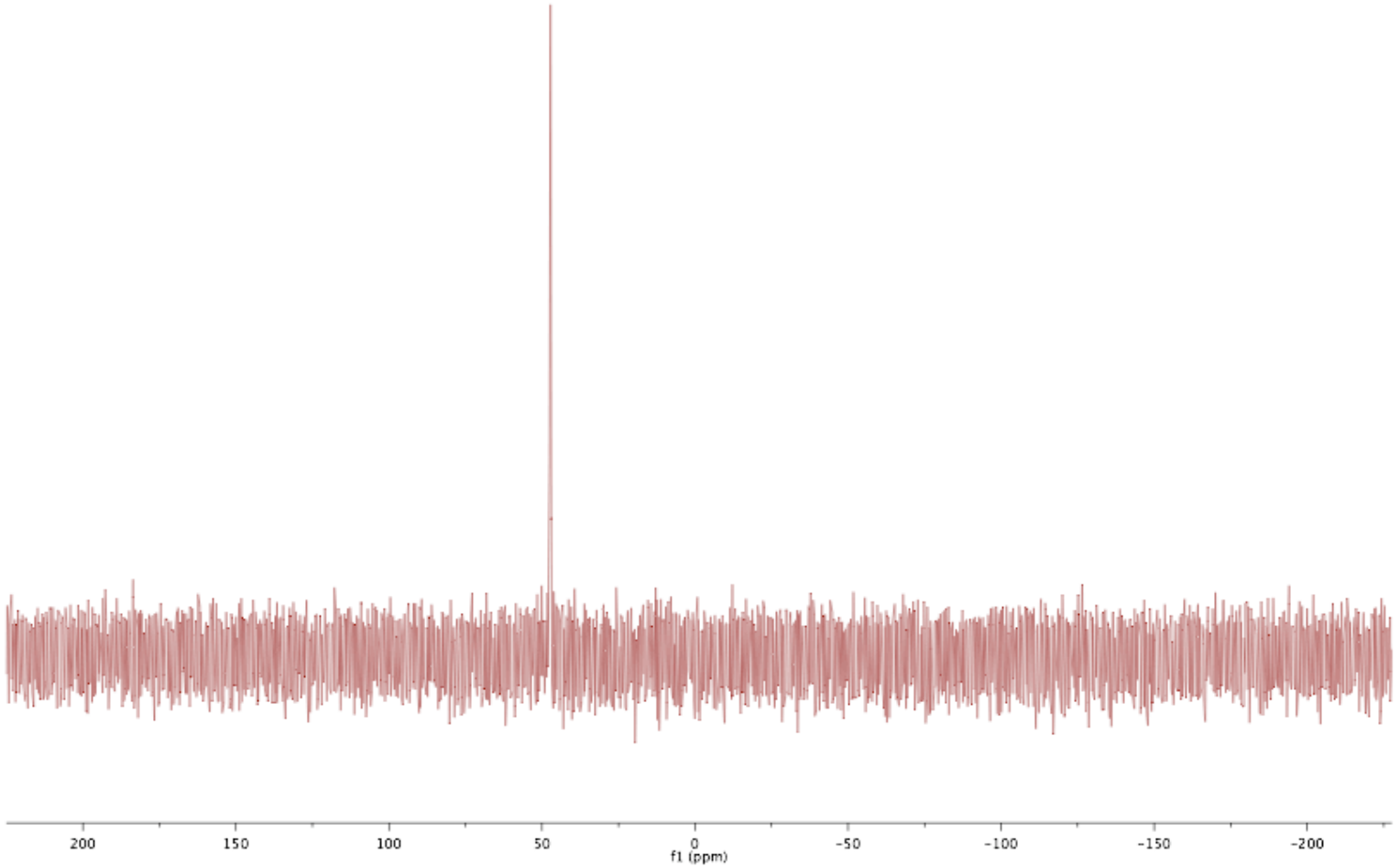

Figure 15. $^{31}P\{^{1}H\}$ NMR spectrum of **3** in C_6D_6

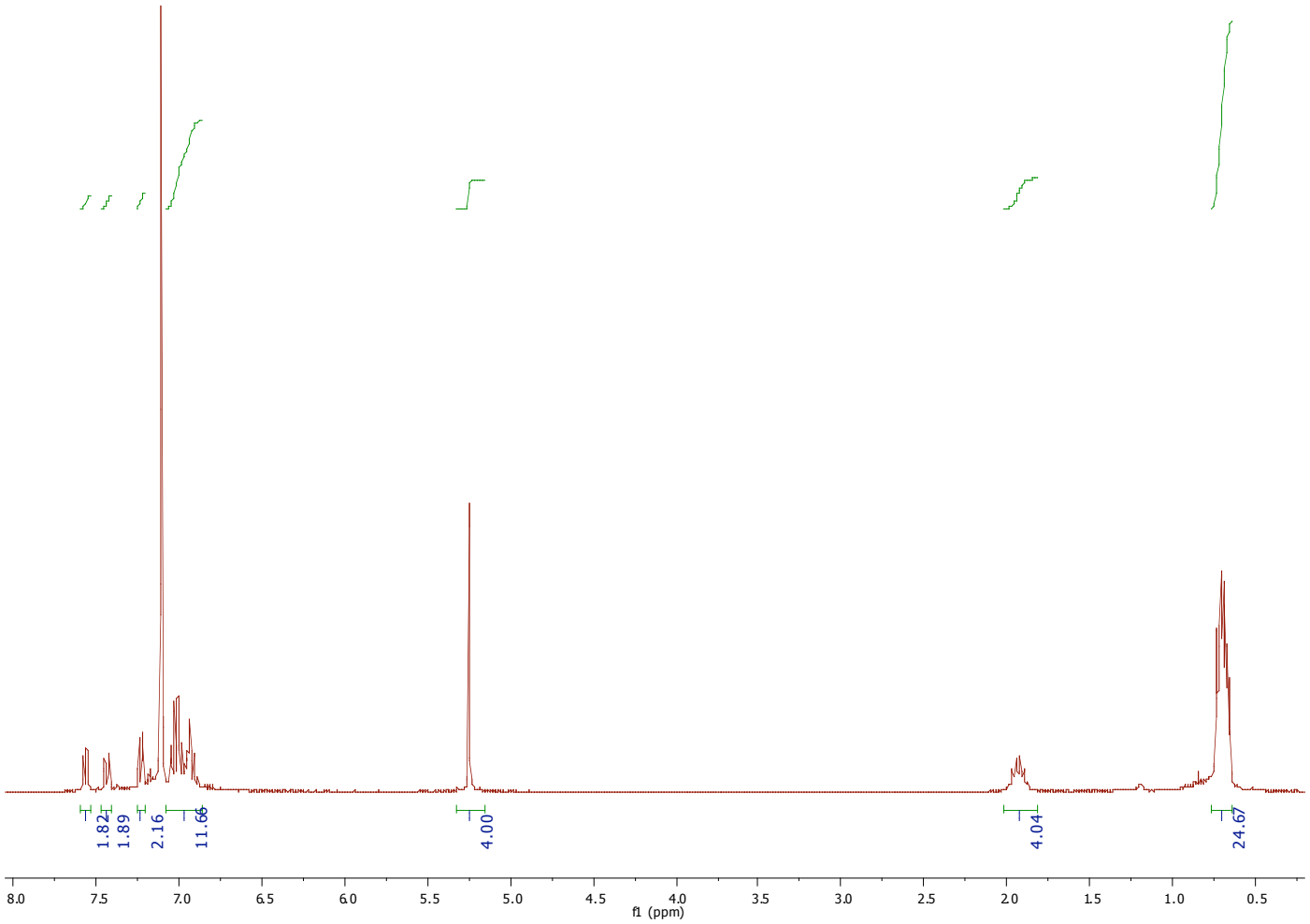

Figure 16. ^{1}H NMR spectrum of **4** in C_6D_6

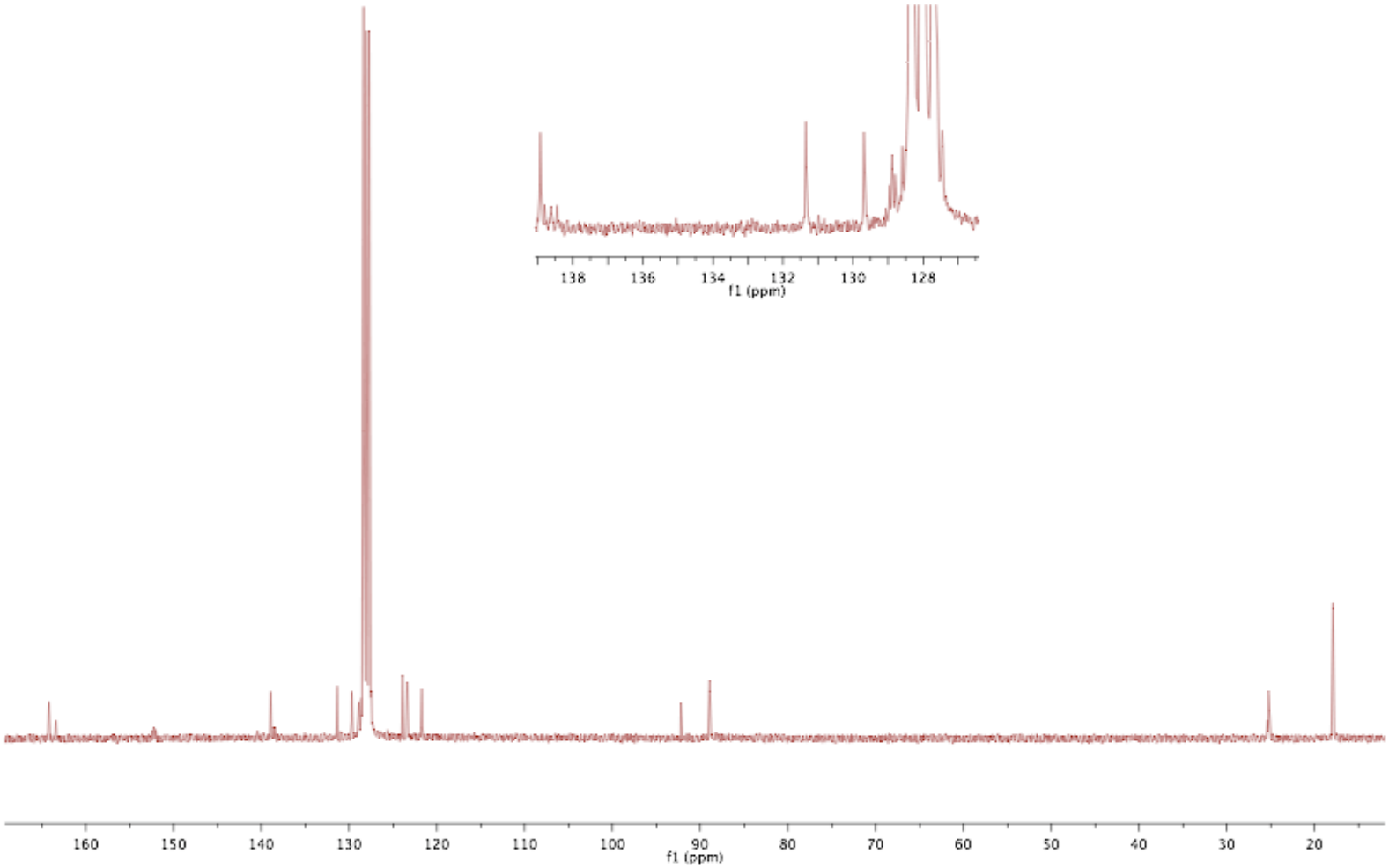

Figure 17. $^{13}C\{^{1}H\}$ NMR spectrum of **4** in C_6D_6

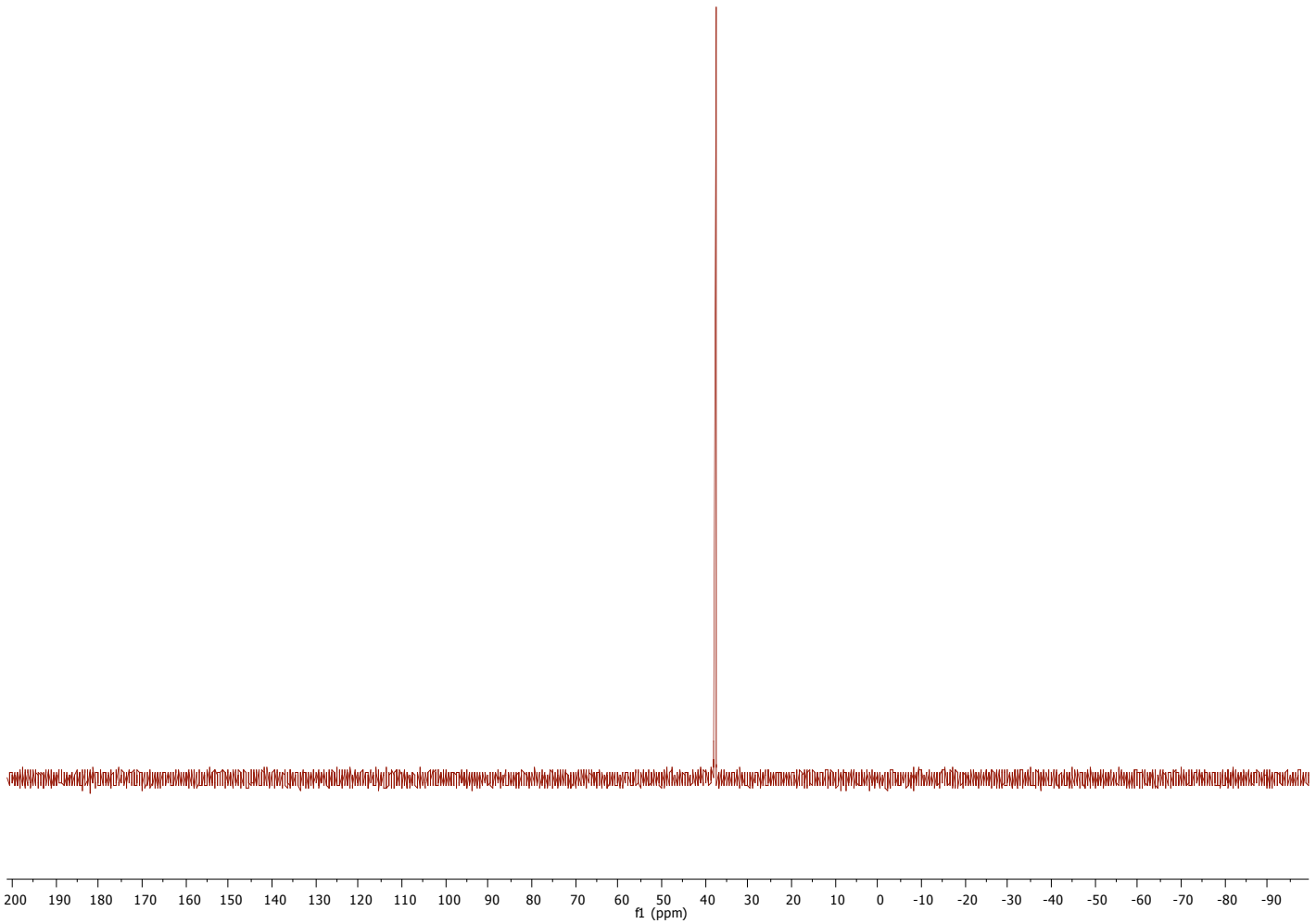

Figure 18. $^{31}P\{^{1}H\}$ NMR spectrum of **4** in C_6D_6

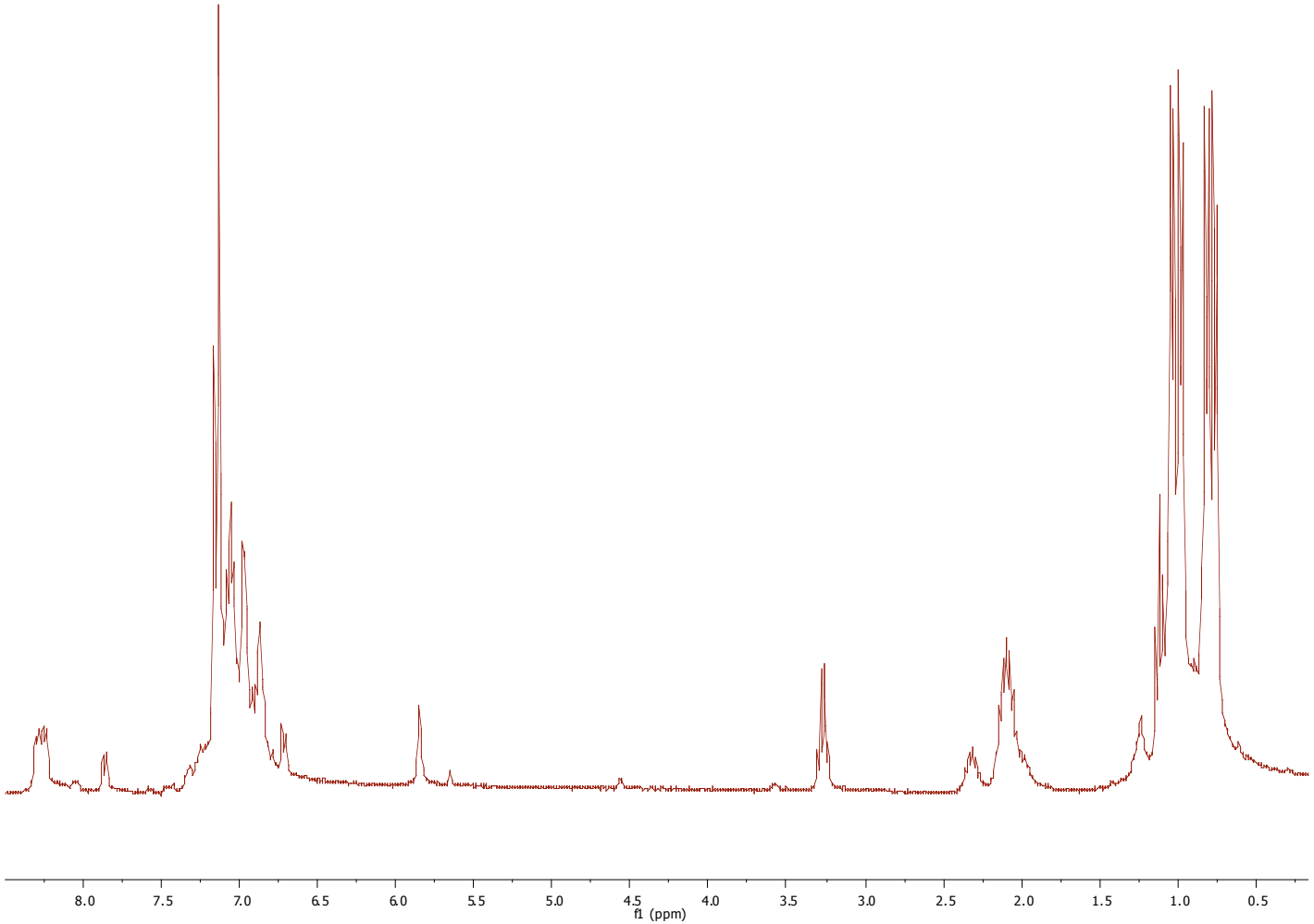

Figure 19. ^{1}H NMR spectrum (C_6D_6) of the mixture derived from the reaction of **4** and 6 equivalents of CO

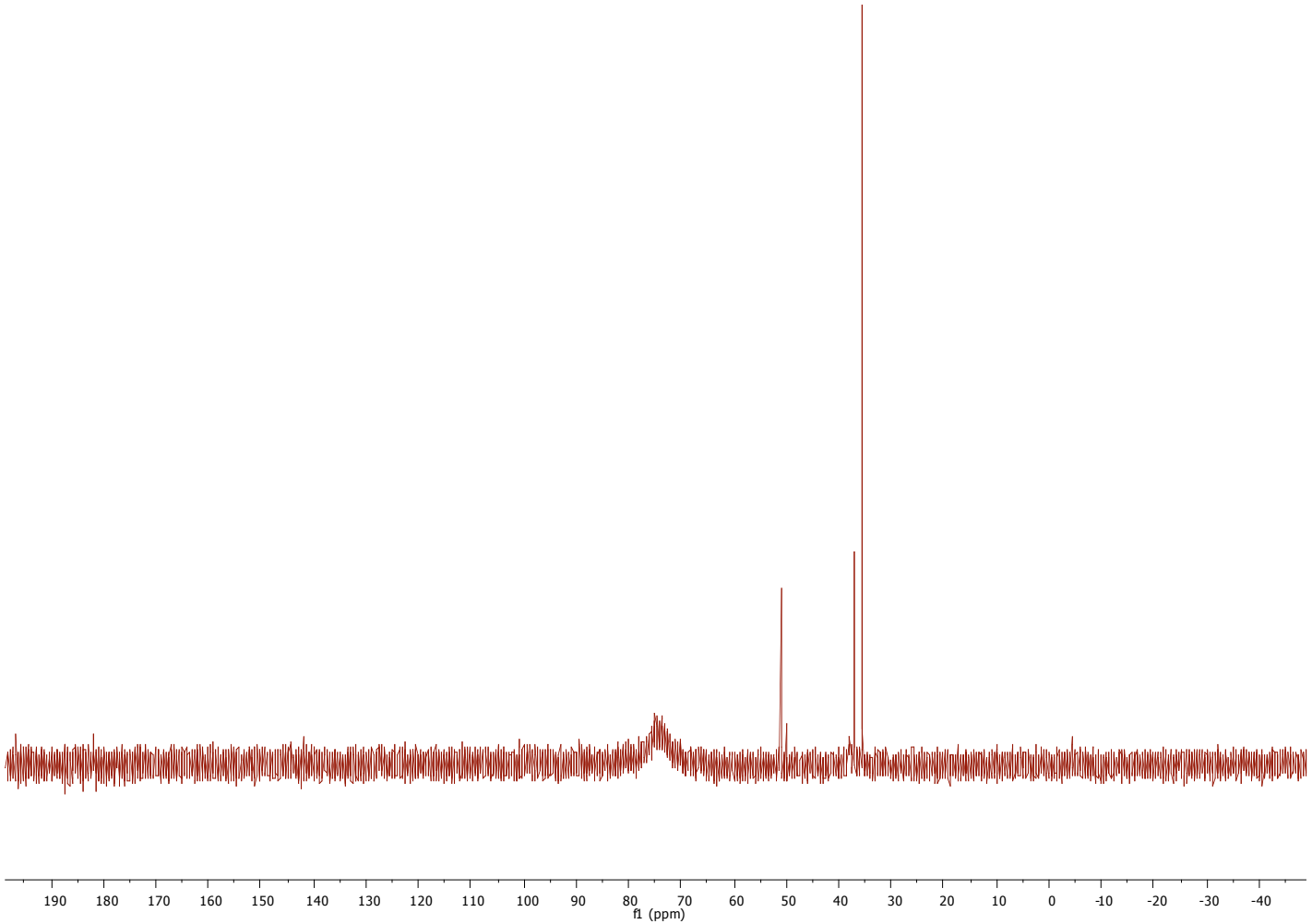

Figure 20. $^{31}P\{^{1}H\}$ NMR spectrum (C_6D_6) of the mixture derived from the reaction of **4** and 6 equivalents of CO

References

(1) Pangborn, A. B.; Giardello, M. A.; Grubbs, R. H.; Rosen, R. K.; Timmers, F. J. *Organometallics* **1996**, *15*, 1518-1520.

(2) Feng, X.; Pisula, W.; Mullen, K. *J. Am. Chem. Soc.* **2007**, *129*, 14116-14117.

(3) Debroy, P.; Lindeman, S. V.; Rathore, R. *J. Org. Chem.* **2009**, *74*, 2080-2087.